Plant, Cell & Environment

Plant, Cell and Environment (2017) **40**, 1456–1473 doi: 10.1111/pce.12942

Original Article

Unravelling early events in the *Taphrina deformans–Prunus persica* interaction: an insight into the differential responses in resistant and susceptible genotypes

Laura A. Svetaz[1,4†], Claudia A. Bustamante[1†], Camila Goldy[1,5], Nery Rivero[1], Gabriela L. Müller[1], Gabriel H. Valentini[2], Alisdair R. Fernie[3], María F. Drincovich[1] & María V. Lara[1]

[1]*Centro de Estudios Fotosintéticos y Bioquímicos (CEFOBI), Facultad de Ciencias Bioquímicas y Farmacéuticas, Universidad Nacional de Rosario, Suipacha 5312000 Rosario, Argentina,* [2]*Estación Experimental San Pedro, Instituto Nacional de Tecnología Agropecuaria (INTA), Ruta Nacional no. 9 Km 170, San Pedro, Argentina,* [3]*Planck-Institut für Molekulare Pflanzenphysiologie, Am Mühlenberg 114476 Potsdam-Golm, Germany,* [4]*Farmacognosia, Facultad de Ciencias Bioquímicas y Farmacéuticas, Universidad Nacional de Rosario, Rosario, Argentina and* [5]*Instituto de Biología Molecular y Celular de Rosario (IBR-Consejo Nacional de Investigaciones Científicas y Técnicas), Facultad de Ciencias Bioquímicas y Farmacéuticas, Universidad Nacional de Rosario, Rosario, Argentina*

ABSTRACT

Leaf peach curl is a devastating disease affecting leaves, flowers and fruits, caused by the dimorphic fungus *Taphrina deformans*. To gain insight into the mechanisms of fungus pathogenesis and plant responses, leaves of a resistant and two susceptible *Prunus persica* genotypes were inoculated with blastospores (yeast), and the infection was monitored during 120 h post inoculation (h.p.i.). Fungal dimorphism to the filamentous form and induction of reactive oxygen species (ROS), callose synthesis, cell death and defence compound production were observed independently of the genotype. Fungal load significantly decreased after 120 h.p.i. in the resistant genotype, while the pathogen tended to grow in the susceptible genotypes. Metabolic profiling revealed a biphasic re-programming of plant tissue in susceptible genotypes, with an initial stage co-incident with the yeast form of the fungus and a second when the hypha is developed. Transcriptional analysis of *PR*s and plant hormone-related genes indicated that pathogenesis-related (PR) proteins are involved in *P. persica* defence responses against *T. deformans* and that salicylic acid is induced in the resistant genotype. Conducted experiments allowed the elucidation of common and differential responses in susceptible versus resistant genotypes and thus allow us to construct a picture of early events during *T. deformans* infection.

Key-words: biotrophic; defensin; dimorphism; flavonoids; leaf curl disease; peach tree; salicylic acid.

INTRODUCTION

Taphrina deformans (Berk.) Tul. is a biotrophic fungus causal of the 'leaf peach curl disease' (Mix 1935), which in addition to leaves can also infect flowers and fruits. It is a devastating and economically important fungal pathogen of peach, nectarine and almond orchards in most of the cultivated areas of these species (Çmen & Ertugrul 2007). In years of severe infection, leaves fall prematurely, and this extensive defoliation corresponds to reductions in yields, higher susceptibility to frost and opportunistic pathogens, and even plant death (Pscheidt 1995). In addition, infected fruits fall prematurely (Rossi *et al.* 2007).

Leaf peach curl disease is characterized by formation of tumour-like structures in leaves and fruits due to cell hyperplasia and hypertrophy (Mehrotra & Aneja 1990). The disease appears at the beginning of spring as reddish areas in developing leaves. These areas got thicker and become curled. Subsequently, affected leaves turn brown or yellow and prematurely abscise (Rossi *et al.* 2007). Other symptoms include leaf spots, leaf curl, deformed fruits and witches' brooms. It is proposed that plant hormonal imbalance due to phytopathogen infection is the cause of tumours due to the capacity of *T. deformans* to synthetize and excrete auxins, as well as cytokinins (Sziràki *et al.* 1975). That said, the exact mechanisms underlying tumour development remain, as yet, unclear (Tsai *et al.* 2014).

Taphrina deformans is a dimorphic ascomycete. The filamentous form characterized by septate hyphae is exclusively found in its host (parasitic), while the yeast form is the saprophytic phase (Rodrigues & Fonseca 2003). There is currently no information on the effectors that prompt the fungal dimorphism, which could be related either to host signals or to ploidy considerations or to both (Nadal *et al.* 2008). Folial anatomy studies revealed that *T. deformans* grows intercellularly either below the cuticle and epidermis or among mesophyll cells. The pathogen present on the lower surface penetrates through the stomata or into the cuticle. *T. deformans* does not form haustoria (Mix 1935). Thus, alteration of interface fungus–leaf cell wall allows pathogen growth. Transmission and scanning electron

Correspondence: M. Valeria Lara; e-mail: lara@cefobi-conicet.gov.ar
[†]*Co-first author*

microscopy accompanied by histochemistry showed that the secretion of polysaccharide-degrading enzymes such as cellulase by the hyphae growing in the intercellular spaces results in a partial dissolution of the plant cell walls. At the interface, the cell wall texture is relaxed, the plant plasma membrane is markedly modified exhibiting vesiculation and the plant middle lamella is dissolved (Bassi *et al.* 1984). Although not tested, the dissolution of the middle lamella suggests the action of other lytic enzymes. In susceptible plants, other ultrastructural differences become evident on pathogen proliferation (Giordani *et al.* 2013).

The study of the resulting disease symptoms through anatomical approaches and of the climatologic conditions favouring the disease (Rossi *et al.* 2007) has received most of the research attention invested in recent years. In contrast, little research has been conducted to elucidate the biochemical and molecular events involved in this interaction. Currently, with the availability of molecular methods that allow the identification of this fungus, there has been a renewed interest in the study of *T. deformans* – as demonstrated by the sequencing of its genome. The *T. deformans* genome encodes enzymes involved in plant cell wall degradation (cellulases, cutinases and xylanases), and many of the proteases that it encodes are predicted to be secreted (Cissé *et al.* 2013).

Resistance to this pathogen is rare; genotype screenings have classified either no or very few cultivars as tolerant (Pscheidt 1995; Padula *et al.* 2008). Thus, understanding the molecular mechanisms underlying leaf peach curl disease resistance is critical to avoid economic losses. Bellini *et al.* (2002) in a programme of controlled crosses analysed more than 200 genotypes. Then selected DOFI 71.043.018 ('Cesarini x Cesarini'), which was tolerant to *T. deformans*. After that, the progeny 'DOFI-84.364' was obtained by self-pollination of DOFI 71.043.018, and then it was crossed with different resistant genotypes giving various selections. Such selection experiments are of great importance, not only to introduce resistance in commercial varieties but also to gain insight into the molecular events involved in the resistance against *T. deformans*, which are currently completely unknown. In the present work, a resistant advanced selection (DOFI-84.364.060) generated by Bellini *et al.* (2002) was investigated, and results were compared with those of two susceptible genotypes.

In order to characterize the metabolic interactions that conduct the disease establishment in susceptible plants or the responses involved in plant resistance in tolerant genotype, early events were examined. For this purpose, for the first time, leaves of *P. persica* were inoculated with *T. deformans* in its yeast phase, and the different phases of fungal colonization were followed up, which included the transition to the filamentous phase. A comprehensive analysis of plant defence responses was accompanied by metabolic profiling of inoculated leaves over a 120 h period. Plant metabolome analyses successfully differentiated between resistant and susceptible genotypes and allowed us to understand metabolic changes upon fungal inoculation. While the hypersensitive response (HR) was observed in all genotypes, differences in defence responses between resistant and susceptible genotypes were observed. Resistance against biotrophic *T. deformans* is associated with the activation of the salicylic acid (SA)-dependent pathway, induction of phenolics and up-regulation of defensin.

MATERIALS AND METHODS

Fungal and plant material

The yeast phase of *T. deformans* (PYCC 5894, Portuguese Yeast Culture Collection, Lisbon, Portugal) was kept on yeast malt agar (YMA) medium [0.3% (*w*/*v*) yeast extract, 0.5% (*w*/*v*) peptone, 1% (*w*/*v*) glucose, 0.3% (*w*/*v*) malt extract and 1.5% (*w*/*v*) agar, pH 5–6] at 22 °C.

Prunus persica L. Batsch trees from the advanced selections DOFI-84.364.089 and DOFI-84.364.060, generated by breeding in University of Florence (Bellini *et al.* 2002), and from cultivar Flavorcrest (FL), were grown at the Estación Experimental Agropecuaria INTA and monitored for at least 5 years. DOFI-84.364.089 (DS) and FL were classified as susceptible to *T. deformans* and DOFI-84.364.060 as resistant (DR).

Experimental design and inoculation

The inoculation of *T. deformans* onto *P. persica* leaves was performed with a blastospore suspension (9×10^6 blastospores mL^{-1}) generated by dilution in H_2Od of 3-day-old culture in YMA. The abaxial surfaces of excised healthy leaves were inoculated with approximately 100 μL blastospore suspension and spreading the inoculum uniformly over the leaf surface. Inoculated leaves were sealed inside humid bags to ensure 100% RH and incubated in a chamber at 22 °C with 16 h light photoperiod for 120 h. Controls were conducted by spreading YMA medium diluted in H_2Od at the same extent as blastopore suspension (mock). Inoculations were conducted under aseptic conditions. Inoculated leaves were harvested at 0, 6, 12, 24, 48, 72, 96 and 120 h post inoculation (h.p.i.) and used for histochemical staining procedures or frozen with $N_{2(l)}$ and kept at −80 °C for further use. Experiments were conducted at least three times (biological replicates) with at least three replicates each.

Histochemical staining procedures

Inoculated leaves were harvested at different time points and clarified in ethanol. Samples were stained with aniline blue for visualization of callose and for staining of the fungal cell wall polysaccharides. Endogenous cell wall autofluorescence allowed the visualization of host tissue. The stained material was viewed with a microscope Nikon Eclipse TE-2000-E2 (Tokyo, Japan) with confocal system Nikon C1Plus SiR using the following settings: excitation = 405 nm and emission = 450 nm. Images were acquired with the Nikon EZ-C1 software.

Accumulation of superoxide was visualized in vacuum-infiltrated leaves with 0.5 mg mL^{-1} NBT (nitro blue

tetrazolium, Promega, Madison, WI, USA) dissolved in buffer phosphate pH 6.8 as a dark blue insoluble formazan compound. Chlorophyll was removed from the leaves before imaging by boiling them in 95% (*v*/*v*) ethanol for 10 min.

The Evans Blue Staining method was used to evaluate cell death (Müller *et al*. 2010).

Pigment analysis

Carotenoids and flavonoids were quantified according to Müller *et al.* (2010). Phenolic compounds and anthocyanins were extracted and quantified as in Cantín *et al.* (2009).

Pathogen growth rate

A DNA-based quantitative real-time PCR (qRT-PCR) method was used to analyse the growth of *T. deformans* in inoculated *P. persica* leaves. Fungal and plant DNAs (DNAg) were extracted from peach leaves following the protocol described by Tavares *et al.* (2004). Ten nanograms of gDNA from *P. persica*-inoculated leaves was used as a template in 20 μL reactions. qRT-PCR was run on the Agilent Mx3000P Real-Time System (Stratagene, La Jolla, CA, USA) and using the intercalation dye SYBR Green I (Invitrogen, Carlsbad, CA, USA) as a fluorescent reporter. The following settings were used: initial denaturation at 95 °C for 3 min and 35 cycles at 94 °C for 20 s, 58 °C for 20 s, 72 °C for 1 min and 72 °C for 3 min. PCR primers ForTd 5′GGTCTCCGGATGGGTTTCAAG3′ and RevTd 5′GCATTTCGCTGCGTTCTTCA3′ were designed based on *T. deformans* internal transcribed spacer 1 (ITS1) sequence published in GenBank (AF492093.1) and using the program 'primer3' (http://www.frodo.wi.mit.edu/cgibin/primer3/primer3_www.cgi). Assays were repeated with three different biological samples. The cycle threshold (C_t) value of *T. deformans* ITS1 gene was compared to that of the plant elongation factor 1α (*PpEF1α*, reference gene) in each sample for which the following primers were used: *EF1αFor* 5′TCCAGTTCTTGATTGCCACA3′ and 5′ *EF1αRev* 5′CCATACCTGCATCTTCGTTC3′, and the relative value for the *T. deformans* titre obtained using the comparative cycle threshold method ($2^{-\Delta\Delta Ct}$). Amounts of *T. deformans* DNA were calculated using the standard curve constructed as follows.

For PCR sensitivity evaluation, the concentration of the fungal DNA template required to obtain reproducible detection in three consecutive assay series was evaluated. To define the limit of detection of the method, 10-fold dilutions from 10 ng to 10 fg of the fungal DNA template were employed. The average of the C_t values was calculated and plotted against the log of the DNA amount to construct the standard curves.

To evaluate the robustness of PCR in biological samples, the same curves described earlier were conducted with the addition of 10 ng of genomic DNA extracted from resistant plants (10 ng).

Gene expression analysis

Three micrograms of total RNA isolated from 40 mg leaves using the TRIzol (Invitrogen) method, MoMLV-reverse transcriptase (Promega) and oligo(dT) was used for cDNA synthesis. Relative expression was quantified by qRT-PCR in an Agilent Mx3000P Real-Time System (Stratagene). Reactions, primer design, controls, PCR specificity confirmation and relative gene expression calculation were conducted as exactly described by Lauxmann *et al.* (2014). Primers used are listed in Supporting Information Table S3. *PpEF1α* was used as the reference gene. Each assay was run in three technical replicates and repeated at least three times using different biological replicates.

Metabolite measurements

Metabolite profiling was assessed by gas chromatography–mass spectrometry (GC–MS) as described by Roessner-Tunali *et al.* (2003). Extraction was conducted as in Lauxmann *et al.* (2014) by using 100 mg of leaf. Ribitol was employed as an internal standard. Mass spectra were cross-referenced with those in the Golm Metabolome Database (Kopka *et al.* 2005). Biological quintuplicates were performed for each stage (h.p.i.) and genotype. Data sets were analysed by principal component analysis (PCA) and Pearson correlation analysis using the XLSTAT package. For data representation, MultiExperiment Viewer software (MeV v4.4.1, http://www.tm4.org/) was used. Data were normalized and expressed as log2 ratios to 0 h.p.i. Metabolite data are reported as Supporting Information according to Fernie *et al.* (2011) (Supporting Information Table S4).

Statistical analysis

Data were analysed using one-way analysis of variance (ANOVA). Minimum significance differences were calculated by the Bonferroni, Holm–Sidak, Dunett or Fisher test ($\alpha = 0.05$) using the SIGMASTAT package. To analyse whether differences among genotypes exist, two-way ANOVA was also conducted.

RESULTS

Leaf inoculation and fungal dimorphism

To gain insight into the mechanisms of fungus pathogenesis and plant responses in the system *P. persica–T. deformans*, we report, for the first time, inoculation experiments to follow the progress of infection. Leaves of a resistant (DOFI-84.364.060, DR) and two susceptible *P. persica* genotypes (DOFI-84.364.089, DS; and Flavorcrest, FL) were inoculated with *T. deformans* in its yeast phase and monitored during 120 h. Over the period analysed, there were no macroscopic differences between mock-inoculated and *T. deformans*-inoculated leaves, denoting that the pre-symptomatic phase is under study in this work (Supporting Information Fig. S1).

To follow the different phases of fungal colonization, confocal microscopy was used (Fig. 1). *T. deformans* dimorphism from the yeast to the filamentous form was achieved after 48 h.p.i. regardless the genotype inoculated (Fig. 1). Septated hyphae, typically of this ascomycete, were observed in all genotypes. In addition, in the section corresponding to a leaf from DS at 120 h.p.i., it is illustrated how the fungus gained ingress into leaves through stomatal openings (Fig. 1); similar results were obtained with leaves of *P. persica* cv. Flavorcrest (not shown). As expected, in control leaves from all genotypes, no fungal development was observed, indicating that leaves were healthy before inoculation. In addition, there were no significant differences between the leaves of any genotypes before inoculation.

Besides monitoring infection by confocal microscopy, we developed an assay of quantitative real-time PCR to quantify the amount of *T. deformans* DNA in the inoculated leaves based on specific amplification of a fragment of *T. deformans* ITS1 gene and the comparison with that of *P. persica* EF1α as an internal reference. Serial dilution (in water) and amplification of *T. deformans* genomic DNA using specific primers for ITS1 gene under the standard real-time PCR conditions demonstrated that the PCR was able to detect 10 fg of fungal DNA (Fig. 2A, black circles). The sensitivity of the reaction was not significantly affected by the addition of 10 ng of background plant DNA (Fig. 2a, grey squares). That is, there were no statistically significant differences ($P < 0.05$) between the slopes of the standard curves conducted with and without the addition of plant DNA. Similarly, cycle threshold (C_t) values of plant EF1α (PpEF1α) were not influenced by the addition of different amounts of fungal DNA (Fig. 2b).

After the sensitivity and robustness of the assay were established, a calibration curve was constructed (Fig. 2c). Finally, total DNA extracted from *P. persica* leaves at different hours post inoculation with *T. deformans* was tested in each host genotype to measure the spread of the fungus (Fig. 2d). In both susceptible genotypes, a biphasic curve is observed, with a maximum at 24 h.p.i. when the fungus is as yeast and then decreasing at 72 h.p.i. and thereafter increasing from 96 h.p.i., when *T. deformans* is present in the filamentous form. In contrast, in the resistant DR, the amount of *T. deformans* only increases at 72 h.p.i., declining afterwards (Fig. 2d).

Prunus persica defence responses

For the examination of the initial histological responses associated with *T. deformans–P. persica* interaction, superoxide production was evaluated histochemically in leaves challenged with *T. deformans*. As shown in Supporting Information Fig. S2, insoluble formazan blue deposition occurred in the three genotypes under study. Nevertheless, the increase in superoxide is earlier in leaves of DR (starting at 24 h.p.i.) than in DS and FL. Evans-blue-stained leaves were used to evaluate cell integrity during the 120 h period after inoculation. Cell death was visualized after 24 h.p.i. in all the samples analysed (Supporting Information Fig. S3). No differences among either genotypes or h.p.i. were observed.

Aniline blue staining was used to disclose callose deposition (Fig. 1). Callose is a highly dynamic cell wall component, frequently somewhat transient in nature. It is involved in a wide range of cell processes such as constituting a physical barrier at sites of infection that restricts the fungal spread (Chen & Kim 2009). Intense fluorescence is observed in the epidermis of inoculated leaves (DS and DR, Fig. 1a, and FL, not shown), with major regions of fluorescence in guard cells, highlighting cell wall thickening around the stomatal pore. Qualitative analysis of images revealed no differences in the

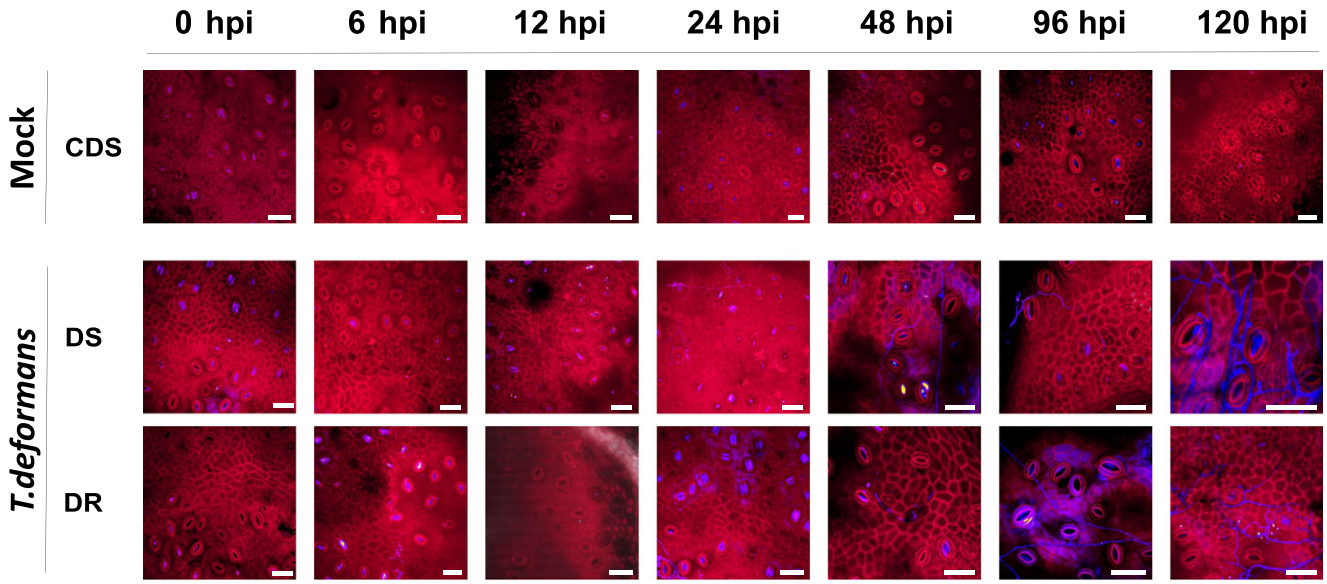

Figure 1. *Prunus persica* inoculation with *Taphrina deformans* in its yeast phase. Leaves were collected after different hours post inoculation (h.p.i.). As controls, mock-inoculated leaves of DS genotype (CDS) are shown. DS, DOFI-84.364.089; DR, DOFI-84.364.060; FL, Flavorcrest. Abaxial side of the leaf is shown. Confocal sections of *P. persica* leaves inoculated with *T. deformans* and stained with aniline blue (fungal cell wall glucans and callose staining, blue). Autofluorescence of plant cell walls is shown in red. Bars = 50 μm.

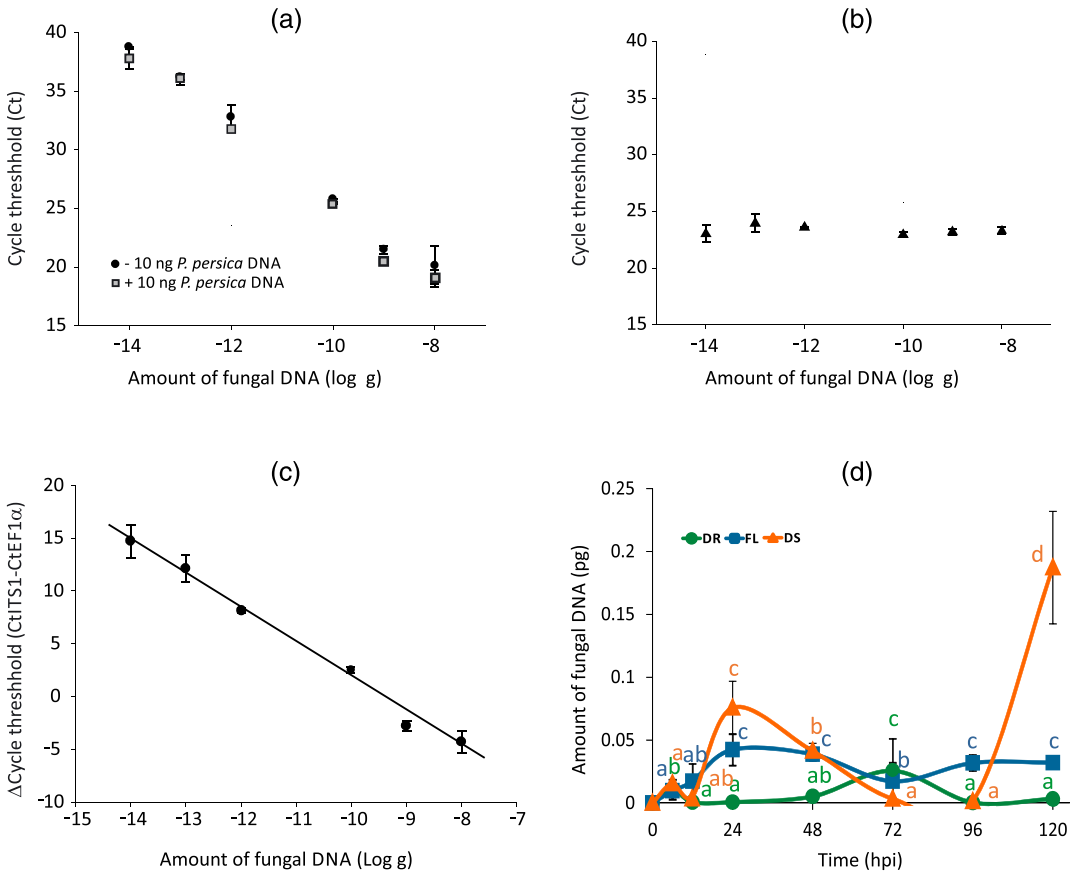

Figure 2. Quantification of *Taphrina deformans* in leaves of different genotypes of *Prunus persica* after inoculation. (a) Relationship between the cycle threshold (C_t) amplification of *T. deformans* internal transcribed spacer 1 (*ITS1*) gene and total fungal DNA. Tenfold dilutions series of fungal DNA were used to cover a range from 10 fg to 10 ng (black circles). The same curve was conducted in the presence of 10 ng of background DNA from plant (black squares). Values represent the mean of three independent determinations ± standard deviation (SD). (b) Stability of the cycle threshold (C_t) amplification of *P. persica* elongation factor 1*α* (*EF1α*) gene in 10 ng of plant DNA in the presence of variable amounts of fungal DNA. Values represent the mean of three independent determinations ± SD. (c) Real-time PCR calibration curve. Standard curve acquired with known amounts of total DNA extracted from fungus conducted in the presence of 10 ng of plant DNA (three repetitions per concentration). (d) Quantification of *T. deformans* by real-time PCR amplification of *ITS1* gene in leaves of resistant (DR) and susceptible (DS and FL) plants at different hours after inoculation (h.p.i.) with the fungus in the yeast phase. The error bars represent standard deviation of the mean ($n = 4$). Bars with at least one same letter are not statically significant ($P < 0.05$, Fisher test). DS, DOFI-84.364.089; DR, DOFI-84.364.060; FL, Flavorcrest. [Colour figure can be viewed at wileyonlinelibrary.com]

extent to which callose is deposited in resistant and susceptible genotypes. While some initial fluorescence is observed in mock-inoculated leaves (CDS), which may be a response to leaf detachment, the intensity decreases over the period analysed. By contrast, fluorescence clearly increases over the time in the *T. deformans*-inoculated leaves.

The kinetics of pathogen induction of genes involved in plant defence responses was also explored. Genes encoding pathogenesis-related (PR) proteins are commonly regulated by plants in pathogenic attacks (Van Loon *et al.* 2006). In addition, phenylpropanoid metabolism activation is key to secondary metabolite production of defence-related compounds, with phenylalanine ammonia lyase (PAL) catalysing the first committed step (Ferreira *et al.* 2007). Thus, based on literature on *Prunus*-responding genes (Ziosi *et al.* 2008; Zubini *et al.* 2009; El-kereamy *et al.* 2011) and on plant defence in other species (Ferreira *et al.* 2007), an *in silico* analysis of *P. persica* genome was conducted to identify homologous genes in peach. Preliminary results allowed the identification of the genes expressed in *P. persica* leaves. Therefore, in this work, the relative expression of transcripts encoding the following proteins, lipid transfer protein 1 (LTP1, PR14), PAL1, thaumatin-like protein (TLP1, PR5), catalase (CAT2), defensin 1 (Dfn1, PR12) and ribonuclease-like protein (Pp1.06A, PR10), was assessed by qRT-PCR (Fig. 3). As controls, time course transcript relative expression was evaluated for most of the transcripts in mock-inoculated leaves to seek for putative changes independent of the fungal inoculation (CDR, Supporting Information Fig. S4). The pattern of accumulation of some transcripts in inoculated leaves was similar in all the *P. persica* genotypes (Fig. 3). While *PpTLP1* increases early after inoculation, *PpLTP1* greatly decreases, with both transcripts tending to increase at 120 h.p.i. Moreover, *PpCAT2* is not induced upon *T. deformans* inoculation in the three genotypes. By contrast, *PpDfn1* is exclusively induced in the resistant genotype (DR) at 48 h.p.

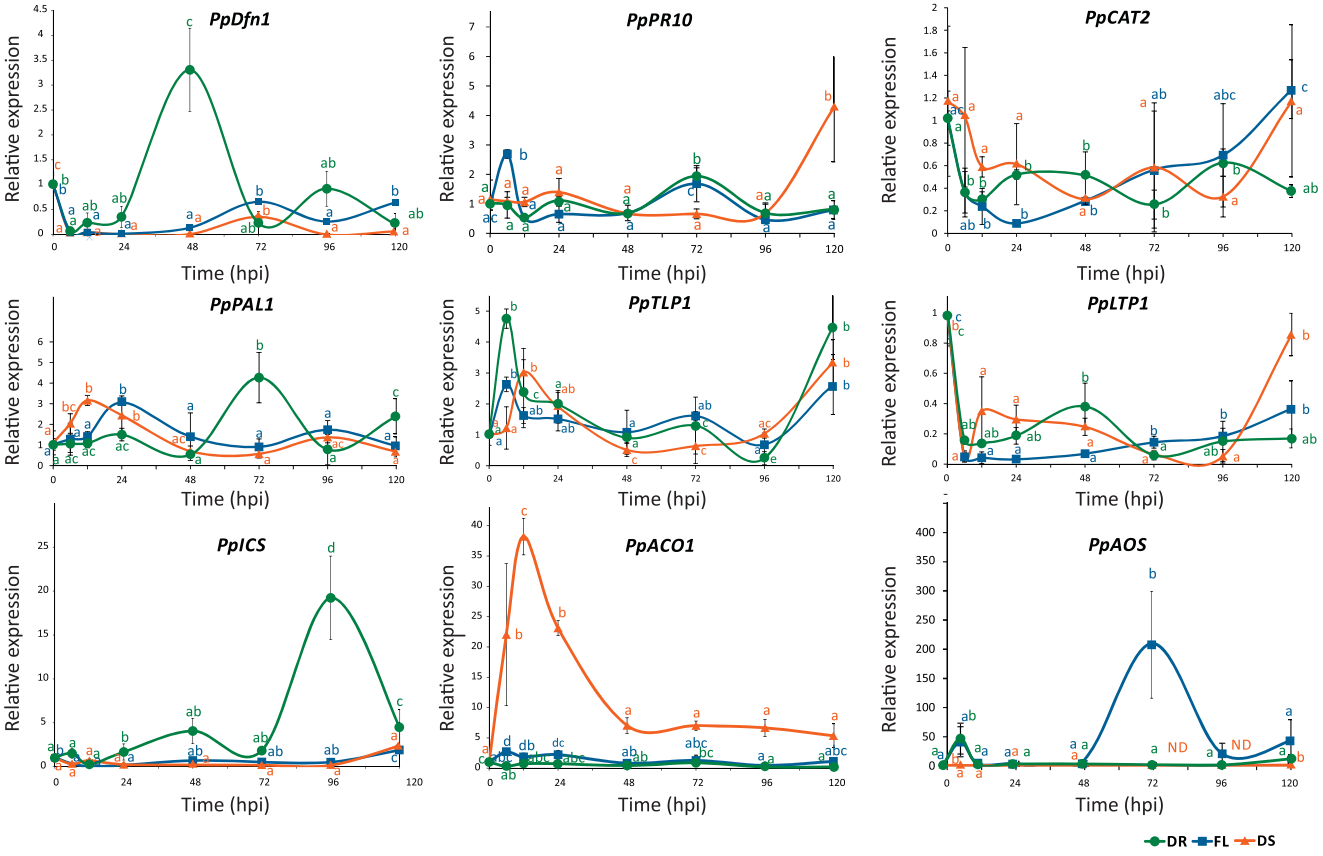

Figure 3. Expression levels of genes involved in plant defence in three different genotypes of *Prunus persica* inoculated with *Taphrina deformans*. Transcript amount was assessed by quantitative real-time RT-PCR, using *P. persica* elongation factor 1α (*PpEF1α*) as the reference gene. *Y*-axes show the fold difference in a particular transcript level relative to its amount at 0 h post inoculation (h.p.i.) in the same genotype. Values represent the mean of at least three replicates ± standard deviation (SD). Bars with at least one same letter are not statically significant ($P < 0.05$). DS, DOFI-84.364.089; DR, DOFI-84.364.060; and FL, Flavorcrest inoculated with *T. deformans*. [Colour figure can be viewed at wileyonlinelibrary.com]

i., and *PpPR10* is differentially induced depending on the genotype, showing significant rises at 6 and 72 h.p.i. in FL, at 72 h.p.i. in DR and at 120 h.p.i. in DS. Regarding *PpPAL1*, there is a significant increase at 72 h.p.i. in DR, while in both susceptible genotypes DS and FL, *PpPAL1* is induced earlier and to a lesser extent (Fig. 3).

Hormonal responses are usually associated with either biotrophic or necrotrophic pathogens (Glazebrook 2005). Thus, transcript levels of enzymes involved in various hormone biosynthetic pathways were also evaluated. The pattern of accumulation of isochorismate synthase (*PpICS*) transcripts required for SA biosynthesis revealed a remarkable induction of almost 20 times at 96 h.p.i. with respect to 0 h.p.i. in the resistant plants (DR). Conversely, there was no induction of *PpICS* in DS over the period analysed and a slight increase in FL at 120 h.p.i. (Fig. 3). The expression of *PpACO1* (1-aminocyclopropane-1-carboxylate oxidase 1) was used as an ethylene production marker. *PpACO1* was repressed in the resistant plants upon inoculation. By contrast, the transcripts were accumulated in the susceptible plants with a maximum of 38-fold in DS at 12 h.p.i. and of 2.7-fold in FL at 6 h.p.i. (Fig. 3). Finally, *PpAOS* encoding an allene oxide synthase (AOS), which is a key step in jasmonic acid (JA) synthesis, was induced nearly 200 times in FL at 72 h.p.i. with respect to 0 h.p.i. and 50 times in DR with respect 0 h.p.i. Conversely, *PpAOS* decreased between 6 and 96 h.p.i. in DS (Fig. 3). Collectively, these results suggest that SA may be involved in signalling events in the resistant genotype but not in the susceptible ones in response to *T. deformans*. Susceptible genotypes also exhibit a differential hormonal response; while ethylene would be induced in DS, JA would be activated in FL.

As means of evaluating plant defence responses, secondary metabolites, such as phenolic compounds (which include flavonoids and anthocyanins) and carotenoids were also quantified (Fig. 4). Total phenolics decreased in all genotypes during the first 24 h. Nevertheless, resistant plants (DR) exhibited an induction at 96 h.p.i. Regarding anthocyanins, increases of sixfold and 9.8-fold were observed at 12 h.p.i. with respect to 0 h.p.i. in DR and FL inoculated leaves, respectively. With respect to flavonoids, the higher levels of these compounds in leaves of DR before and after inoculation with respect to susceptible genotypes were notable; DR flavonoids at 0 h.p.i. are about 2.5-fold the levels in DS. This fact notwithstanding, all genotypes show a maximum of flavonoids at 96 h.p.i. (Fig. 4). On the other hand, carotenoids exhibited a rapid response, although of a smaller magnitude, increasing in

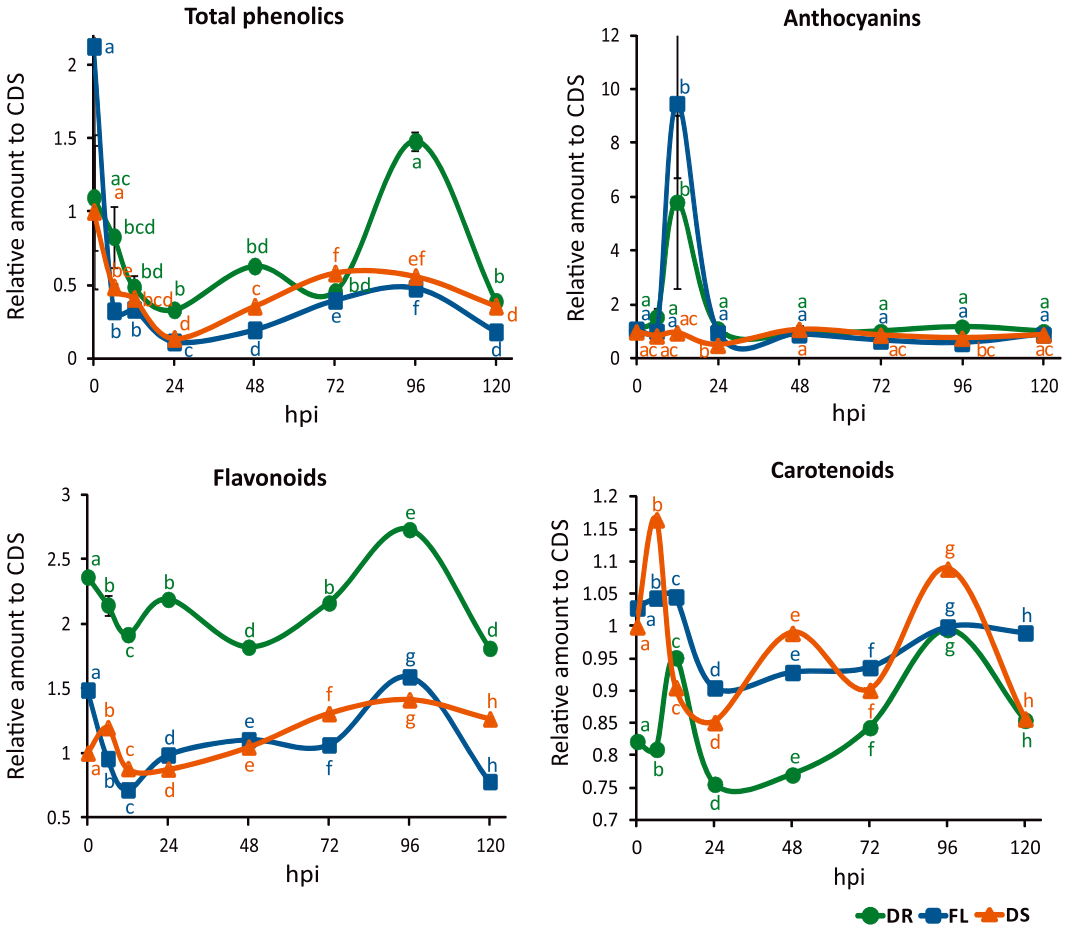

Figure 4. Changes in leaf pigments composition after inoculation. Carotenoid, flavonoid, anthocyanin and phenolic compounds are expressed in relation to the values of control DS leaves (CDS) at each time. The error bars represent standard deviation of the mean ($n = 3$). Bars with at least one same letter are not statically significant ($P < 0.05$). DS, DOFI-84.364.089; DR, DOFI-84.364.060; and FL, Flavorcrest inoculated with *Taphrina deformans*. [Colour figure can be viewed at wileyonlinelibrary.com]

all genotypes at 6–12 h.p.i. with a second peak being observed at 96 h.p.i. (Fig. 4).

Primary metabolism in leaves of *Prunus persica* challenged with *Taphrina deformans*

Gas chromatography–MS analyses of leaves from the three genotypes (DR, DS and FL) resulted in the identification of 50 metabolites, which were grouped according to their biochemical properties and functions as amino acids, organic acids, sugars, alcohol sugars, fatty acids or miscellaneous compounds. Amounts of each metabolite were determined in biological quintuplicates and estimated in relation to ribitol, which was added as an internal standard. Normalized metabolite levels were expressed relative to the values measured in CDS (control leaves of non-inoculated DS) at each corresponding time after inoculation. Results are summarized in Supporting Information Table S1. Figure 5 represents the relative metabolite levels and shows the changes in the metabolome with the time of inoculation. While some responses are common to all genotypes, as is the case of miscellaneous compounds such as spermidine and urea, other variations are only shared by the susceptible genotypes (DS and FL), and not by DR, as is the case of some sugars (raffinose and sucrose) and amino acids (Asn, Trp and Tyr). In general and regardless the genotype, a biphasic response can be observed in the levels of all metabolites, with an early phase around 6 and 24 h.p.i. and a later response centred at 96 h.p.i.

The metabolite profiles assessed by GC–MS were subjected to PCA (Fig. 6), which showed the three highest-ranking principal components (PCs) accounted for 57.8% of the total variance within the data set. PC1, PC2 and PC3 accounted for 26.8, 19.58 and 11.27% of total variance, respectively. PCA could clearly differentiate samples from susceptible genotypes (DS and FL) and those from the resistant plants (DR), especially in graphs PC1 versus PC2 and PC1 versus PC3. Supporting Information Table S2 depicts the contribution of individual variables to each PC. Compounds that contribute the most to each component are shown in Fig. 6.

Metabolite–metabolite correlation analysis was pursued by using Pearson's correlation coefficients (Supporting Information Fig. S5). Out of 1225 pairwise correlations, 422 resulted in significant correlation coefficients ($P > 0.5$). While

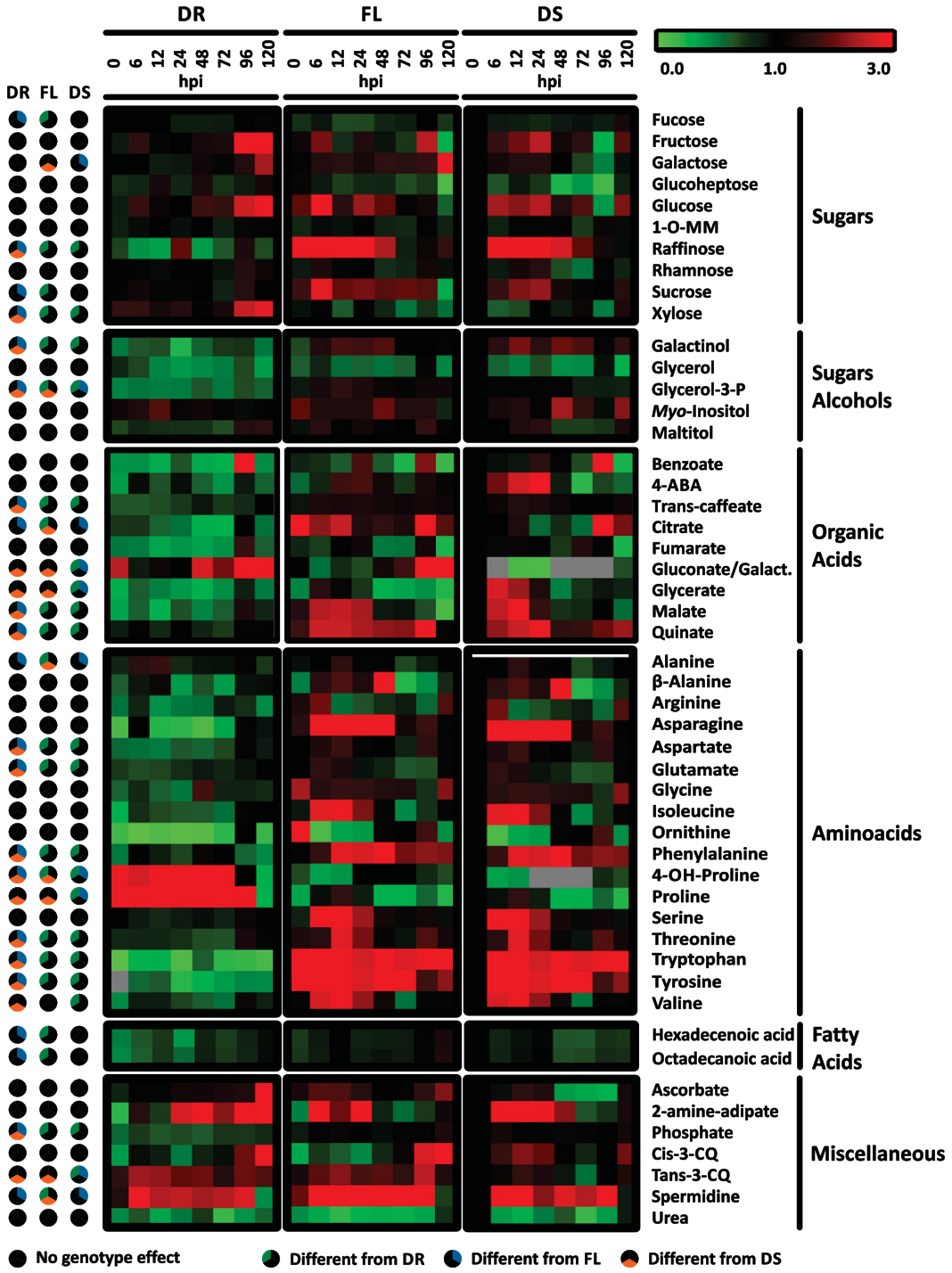

Figure 5. Metabolite profiling of *Prunus persica* leaves challenged with *Taphrina deformans*. The graph shows the amounts of each metabolite in DR, DS and FL across the 120 h after inoculation with the fungus in relation to the level determined in control mock-inoculated DS leaves (CDS) at the same hours post inoculation (h.p.i.). Normalized values are presented by using a colour scale proportional to the level of each metabolite (shown at the top of the figure). Heat map was created using MEV 4.1. Relative values for each metabolite peak area are provided in Supporting Information Table S1. Values are the mean of five biological independent determinations expressed in relation to the values in CDS at each corresponding time. Red and green indicate metabolite levels in leaves challenged with *T. deformans* greater and lower, respectively, than those in the control leaves (CDS). Results from the analysis of the genotype effect on metabolite variations by two-way ANOVA are shown schematically on the left of the figure. The colour of each circle indicates whether there are differences in the metabolite profile across time in the genotype indicated in the column with respect to the other genotypes tested (i.e. black stands for the absence of genotype effect, green indicates different from DR, red denotes different from DS and blue represents that the behaviour differs from that of FL. DS, DOFI-84.364.089; DR, DOFI-84.364.060; and FL, Flavorcrest challenged with *T. deformans*. Cis-3-CQ, *cis*-3-caffeoyl-quinic acid; 1-O-MM, 1-*O*-methyl mannopyranoside; Trans-3-CQ, *trans*-3-caffeoyl-quinic acid; GABA, 4-amine-butyrate; gluconate/galactonate. [Colour figure can be viewed at wileyonlinelibrary.com]

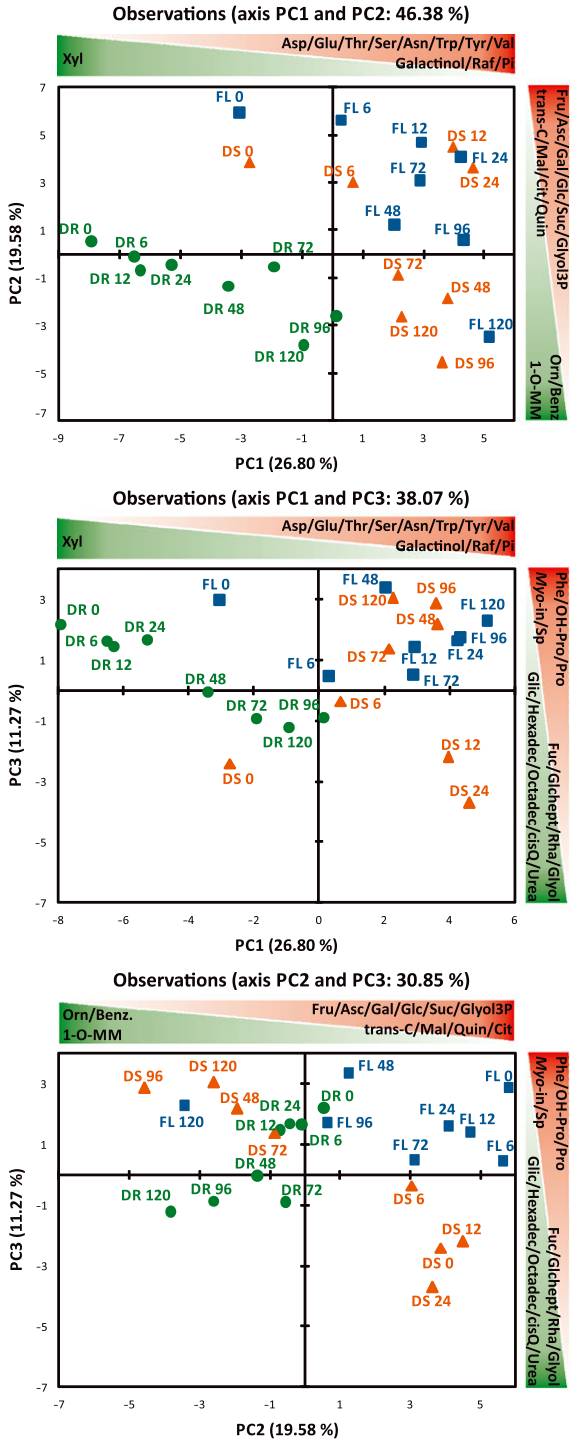

Figure 6. Principal component analysis (PCA) score plot of leaves of susceptible and resistant genotypes inoculated with *Taphrina deformans* and analysed by gas chromatography–mass spectrometry (GC–MS). Variance explained by each component (%) is shown in parentheses. Metabolites, which contribute the most to each component, are shown in red (positive contribution) and green (negative contribution). The number at the right of each name denotes the hours post inoculation (h.p.i.) of each sample; that is, DS72 stands for DS analysed at 72 h.p.i. DS, DOFI-84.364.089; DR, DOFI-84.364.060; and FL, Flavorcrest challenged with *T. deformans*. CDS, mock-inoculated control DOFI-84.364.089 leaves. [Colour figure can be viewed at wileyonlinelibrary.com]

308 coefficients of these were positive in nature, 114 were negative.

Metabolome analysis of leaves challenged with *T. deformans* revealed that in susceptible genotypes (DS and FL) the amino acids display a similar profile (Figs 5 & 7) with two peaks of increase over the inoculation period. Among amino acids with this behaviour, two groups can be distinguished. In the first group Asp, Glu, Ser, Thr and Val increase from 1.5-fold to fourfold between 6 and 12 h.p.i. and then show a second peak of 1.5-fold to twofold increase at 96 h.p.i. In the other group composed of Asn, Phe, Tyr and Trp, the second peak is closer to the first peak, at 48 h.p.i., except for Asn that occurs at 24 h.p.i.; in addition, this second group exhibits higher increases (between fivefold and 80-fold). By contrast, in leaves of resistant plants (DR), neither an earlier induction (i.e. Asp, Ser, Thr, Val and Orn) nor change was observed. Moreover, the levels of most amino acids before inoculation (0 h.p.i.) are considerably lower in the resistant genotype DR than in susceptible plants (DS and FL, Fig. 7; i.e. Asp and Trp). On the other hand, Pro levels differs in the susceptible DS from FL and from DR (Figs 5 & 7).

Regarding sugars, for some metabolites, the same behaviour is observed in both resistant and susceptible leaves, as it is the case of rhamnose and 1-*O*-methyl-mannopyranoside. In other cases, such as fructose, the tendency is to increase towards the end of the period analysed. In the case of xylose, even though a net decrease is observed in all genotypes at 12 h.p.i., on one hand, the relative levels in DR are higher than in both susceptible genotypes and tend to increase towards the end of the period analysed. It is worth noting the case of raffinose, which exhibits a substantial increase of between 30-fold and 80-fold in both susceptible genotypes (DS and FL) while DR displays much lower levels at 0 h.p.i. that remain constant or even decrease during the first days after inoculation (Figs 5 & 7). Sugar alcohols also differ in susceptible plants than in the resistant genotype, as accounted by higher levels (between twofold and fourfold higher) of glycerol-3-P in DS and FL than in DR over the period analysed. On the other hand, in susceptible plants, galactinol doubles (in DS) or triples (in FL) its level at 12 h.p.i. with respect to 0 h.p.i. (Figs 5 & 7).

In the organic acid module, benzoate, 4-amine-butyrate (GABA) and fumarate levels exhibit two peaks across the inoculation period but do not display genotype effects. Regarding glycerate, an early peak at 6 h.p.i. is observed in the three genotypes; and a second increase of 2.7 times is registered only in DR at 96 h.p.i. On the other hand, citrate depicts a peak at 96 h.p.i, which is of higher magnitude in susceptible plants than in DR (4.3-fold, 2.1-fold and 1.4-fold increase with respect to 0 h.p.i. in DS, FL and DR, respectively). Conversely, malic, quinic and *trans*-caffeic acids differ in resistant plants with respect to susceptible ones. Particularly, malate increases twofold and threefold in DS and FL, respectively, at 12 h.p.i., while the resistant plants' induction of about four times with respect to 0 h.p.i. occurs later at 96 h.p.i. (Figs 5 & 7).

Despite mild variations in the fatty acid profile, there were no remarkable differences unique to the susceptible or resistant plants (Figs 5 & 7).

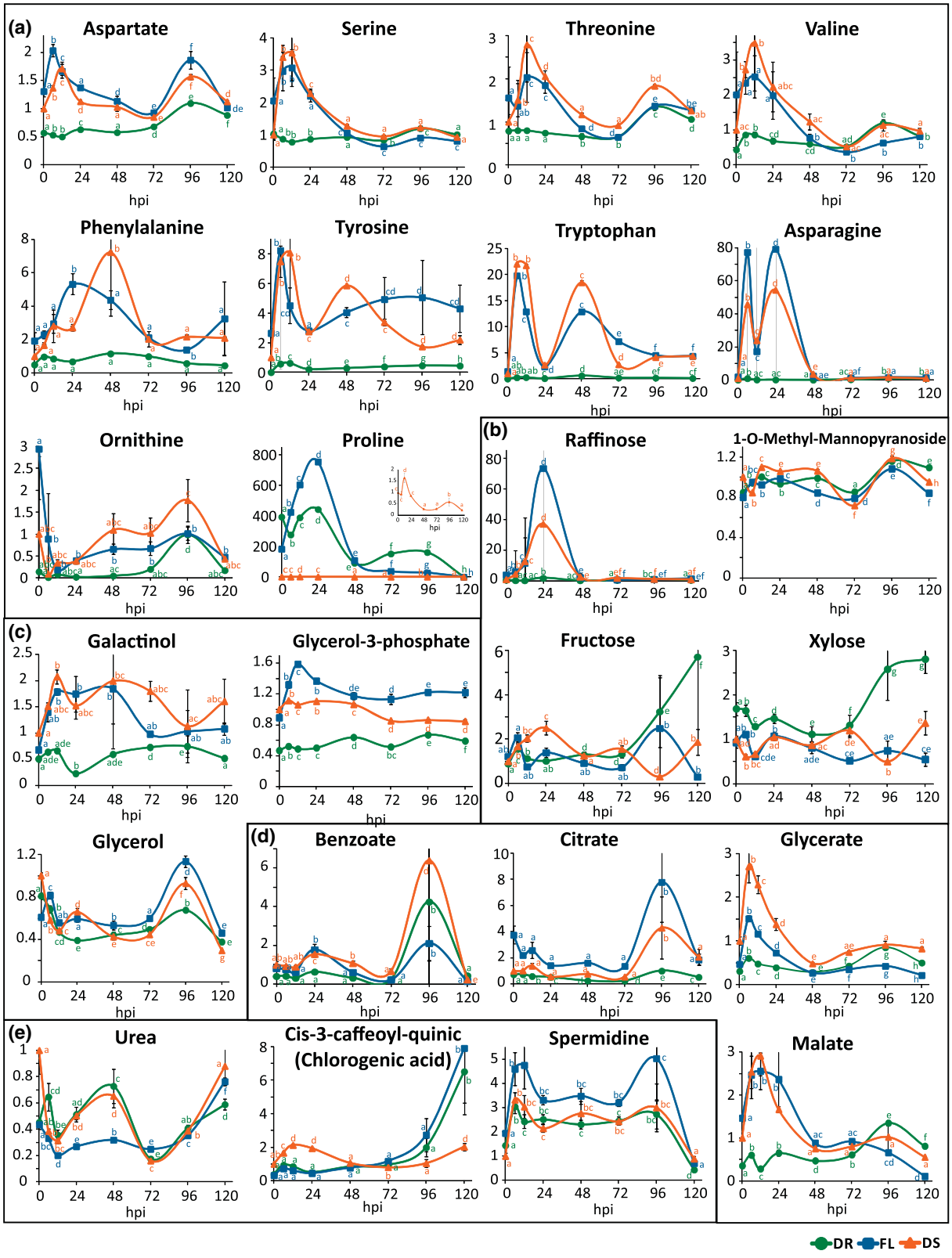

Figure 7. Metabolite concentration changes in *Prunus persica* leaves challenged with *Taphrina deformans*. Graphs show the levels of each metabolite (mean of five biological independent determinations) in inoculated leaves in relation to the value (mean of five biological independent determinations) in control leaves (CDS) at the same time post inoculation (h.p.i.). Error bars represent standard deviation (SD). For each parameter, values with at least one same letter are not significantly different ($P < 0.05$). Metabolites are presented by groups: (a) amino acids; (b) sugars; (c) sugar alcohols; (d) organic acids; and (e) miscellaneous. DS, DOFI-84.364.089; DR, DOFI-84.364.060 and FL, Flavorcrest challenged with *T. deformans*. CDS, mock-inoculated control DOFI-84.364.089 leaves. [Colour figure can be viewed at wileyonlinelibrary.com]

Regarding the miscellaneous compounds, chlorogenic acid (*cis*-3-caffeoyl-quinic acid) increases about twofold at 12 h.p.i. with respect to 0 h.p.i. and then tends to increase later in all genotypes although at different extents. Spermidine also tends to increase in all genotypes as well but returns to initial levels at 120 h.p.i. Although urea depicts a similar profile in all genotypes analysed, the initial decrease in the susceptible plants is not observed in DR (Figs 5 & 7).

Finally, because raffinose was dramatically induced in susceptible genotypes (DS and FL) upon *T. deformans* inoculation, a comprehensive profiling of transcripts encoding enzymes involved in its metabolism was conducted by qRT-PCR (Fig. 8). In the first step of raffinose biosynthesis, galactinol synthase (GolS) produces galactinol, which is then used by raffinose synthase (RS) to produce the trisaccharide. By contrast, the so-called seed imbibition proteins (SIPs) are galactosidases involved in raffinose catabolism (Lauxmann *et al.* 2014). The time course of transcript expression in FL revealed no significant changes in *PpGolS1* and *PpRS* over the 120 h.p.i. analysed; increases in *PpGolS4* at 72, 96 and 120 h.p.i.; a slight increase of *PpSIP1* at 24 h.p.i.; and a significant decrease of *PpSIP2* upon inoculation with relative values ranging from 5 to 33% of that at 0 h.p.i. A complete different profile was observed in DS, with a twofold increase in *PpRS* at 12 h.p.i., a significant fall in both *PpGolS-1* and *PpGolS-4* upon pathogen inoculation and a prominent induction of both *PpSIP-1* and *PpSIP-2* around 72 and 96 h.p.i. (Fig. 8). Regarding the resistant plant, while *PpGolS4* increased at 6 h.p.i., *PpGolS1* decreased at the same time and remained low, *PpRS*, *PpSIP-1* and *PpSIP-2* remained almost constant over the period analysed (Fig. 8).

Given that Pro accumulated to a great extent in DR and FL, transcripts encoding the enzymes involved in the synthesis of its precursor pyrroline-5-carboxylate (P5C), P5C synthase (*PpP5CS-1* and *PpP5CS-2*) and δ-ornithine aminotransferase (*PpδOAT*) were quantified in both susceptible and resistant plants (Fig. 8). In DR, while *PpδOAT* remained constant, *PpP5CS-1* and *PpP5CS-2* showed increases at 6 h.p.i. (fourfold with respect to 0 h.p.i.) and 72 h.p.i. (10-fold with respect to 0 h.p.i.), respectively. Surprisingly, in FL, *PpδOAT*, *PpP5CS-1* and *PpP5CS-2* declined after *T. deformans* inoculation. Regarding DS, *PpδOAT* (12-fold) and *PpP5CS1* (sevenfold) were induced at 12 h.p.i .with respect to 0 h.p.i., and a second peak at 96 h.p.i. was observed for *PpP5CS1* at 96 h.p.i. *PpP5CS2* did not exhibit significant changes (Fig. 8).

DISCUSSION

The filamentous form of *Taphrina deformans* is developed in *Prunus persica* leaves after inoculation with the yeast phase

Taphrina deformans is the causal agent of peach leaf curl, a disease that affects not only peach and nectarine but also almond orchards around the world (Rossi *et al.* 2007). It is a harmful pathogen that causes important economical loses; however, the dimorphic nature of this fungus has constituted a hindrance to knowledge enlargement of this disease. To understand the interaction between *T. deformans* and its host *P. persica*, a comprehensive analysis of the fungal development and the plant metabolic response was conducted here. Even though all known commercial cultivars are susceptible to this pathogen, an advanced selection breeding approach to yield a resistant line (DOFI-84.364.060) was performed in Italy (Bellini *et al.* 2002), and this line was used in the current work to obtain insight into the factors underlying resistance. On the other hand, to ascertain the metabolic changes associated with pathogen colonization and to discriminate them from biological variation, two susceptible genotypes were employed, Flavorcrest and DS (another member of the same selection

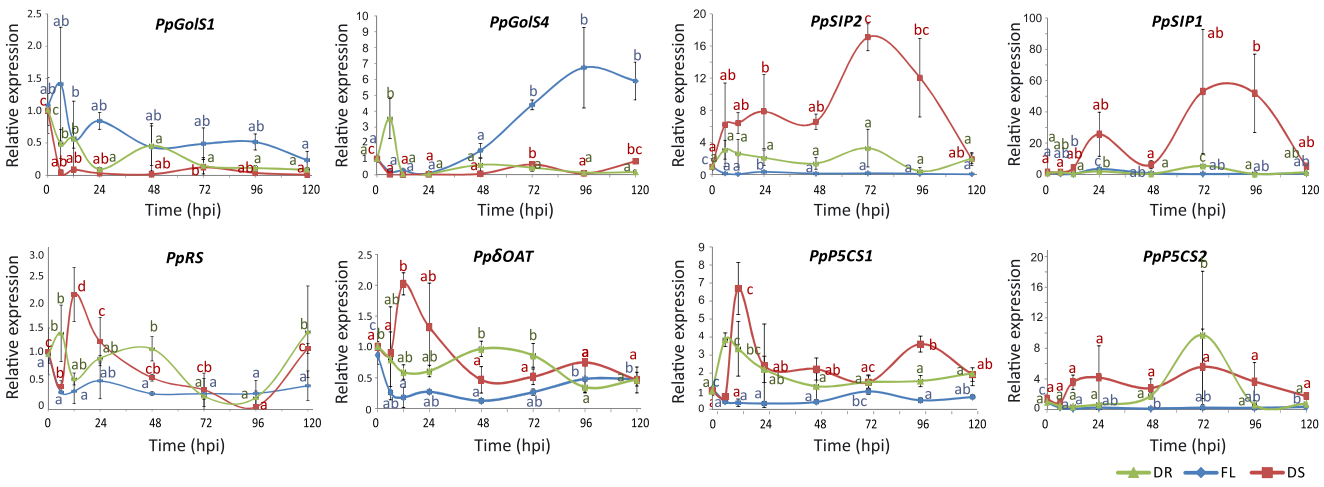

Figure 8. Expression analyses of transcripts encoding enzymes involved in raffinose (*PpGolS-1* and *PpGolS-4*, *PpRS*, *PpSIP-1* and *PpGolS-2*) and proline metabolism (*PpP5CS-1* and *PpGolS-2*, *PpδOAT*) in *Prunus persica* leaves after *Taphrina deformans* inoculation. Means ± standard deviation (SD) of results obtained, using three independent RNAs as template, are shown. The expression level of each gene is relative to that of 0 hours post inoculation (h.p.i.). *PpEF1α* was used as a reference gene. For each transcript analysed, bars with the same letters are not significantly different ($P < 0.05$). DS, DOFI-84.364.089; DR, DOFI-84.364.060; and FL, Flavorcrest challenged with *T. deformans*. [Colour figure can be viewed at wileyonlinelibrary.com]

panel as DR). The aim of this study was to achieve a deep characterization of the early responses upon pathogen inoculation and thus analyse the pre-symptomatic stage of the disease. The absence of leaf hyperplasia or changes in pigmentation in treated leaves (Supporting Information Fig. S1) are evidences that signs of disease are not yet developed during the period analysed. To the best of our knowledge, this is the first time that *P. persica* leaves are inoculated with *T. deformans*, and the progress of infection and plant responses are evaluated during the following 120 h, and fungal dimorphism has been achieved under laboratory conditions. Regardless of the plant genotype, septated hyphae were visualized after 48 h.p.i. (Fig. 1). Many economically important pathogens are dimorphic fungus such as *Magnaporthe grisea* infecting rice, wheat, barley, rice and so on; *Ustilago maydis* infecting maize; and *Mycosphaerella graminicola* affecting wheat (Doehlemann *et al.* 2008; Nadal *et al.* 2008; Gohari *et al.* 2015; McDonald *et al.* 2015; Rudd 2015; Lo Presti *et al.* 2015; Tollot *et al.* 2016). *U. maydis* has become a model species to study fungal pathogenicity and dimorphism. For many of these dimorphic fungi, the transition to the pathogenic state can be mimicked in culture by media modification (Guevara-Olvera *et al.* 1997; Nadal *et al.* 2008). In the case of *T. deformans*, stable hyphal development occurs exclusively in the host tissue, and thus, filamentous form is considered as obligate parasitic. Therefore, the establishment of a system that allows hypha development under controlled laboratory conditions is of great importance.

In comparison with other biotrophs such as *U. maydis*, a pathogen that forms the specialized haustoria for nutrition and grows both inter-cellularly and intra-cellularly, the induction of *T. deformans* dimorphism is more slowly. While after 12 h.p.i., most of the *U. maydis* haploid sporidia used to infect maize had formed hyphae and developed the appressoria (Doehlemann *et al.* 2008), only after 48 h.p.i. did *T. deformans* yeast cells turn into their filamentous form. On the other hand, in both maize–*U. maydis* and *P. persica*–*T. deformans* pathosystems, early plant responses are observed around 12 h.p.i. (Doehlemann *et al.* 2008, Figs 4, 5, 7 & 8).

Early responses are activated in *Prunus persica* in response to *Taphrina deformans* inoculation

Plants safeguard themselves by means of both biochemical and physical defences. During early stages of pathogen invasion, production of reactive oxygen species (ROS) and defence compounds by host tissue is usually accomplished. Here, the superoxide anion accumulated upon *T. deformans* inoculation in all genotypes; this was also accompanied by cell death, with both features indicative of an HR (Supporting Information Figs S2 & S3). In addition, callose deposition was also observed (Fig. 1).

The analysis of the transcriptional responses of genes involved in the biosynthesis of hormones that usually respond to pathogen attack reveals an early induction of *PpAOS* followed by a later activation of *PpICS* in DR to *T. deformans* infection (Fig. 3). Resistance against biotrophic pathogens is frequently regulated by SA, whereas jasmonate-dependent and ethylene-dependent pathway activations are usually associated with resistance to necrotrophic pathogens (Bari & Jones 2009). In DR, *PpICS* induction at 96 h.p.i. parallels the decrease in *T. deformans* (Fig. 2). Because SA acts locally and systemically (Vlot *et al.* 2009), activation of SA synthesis through isochorismate synthase may be efficient against the filamentous form of *T. deformans* and also facilitate systemic acquired resistance in the DR genotype and thus mediate the defence in distal parts of the plant. By contrast, SA appears not to be induced in the FL and DS, a condition that is thus conducive to the disease. In the susceptible genotypes, ethylene-dependent and/or jasmonate-dependent pathways are activated (Fig. 3), but they would be inefficient in fighting against *T. deformans*.

The production of so-called PR proteins (van Loon *et al.* 2006) is another inducible defence mechanism that is activated in *P. persica* upon *T. deformans* attack, as evidenced by the up-regulation of *PpPR10* and *PpTLP-1* (Fig. 3) in both susceptible and resistant genotypes. Members of the PR10 family are known as peach major allergens (Prup1.01 and Prup1.06D) and have also been related to decreased susceptibility to *Monilinia* spp. during stone hardening (Zubini *et al.* 2009). On the other hand, TLPs are β-1,3-glucanases belonging to the PR5 protein family. In leaves of *P. persica*, *PpTLP-1* and *PpTLP-2* were considerably more highly expressed in a cultivar resistant to *Xanthomonas campestris* pv. *pruni* than in a susceptible one in response to bacteria inoculation (Sherif *et al.* 2012). In the case of fruits of *Prunus domestica* challenged with the fungus *Monilinia fructicola*, while the levels of *PdPR5-1* are constitutively higher in the resistant genotypes, the transcript levels promptly increased during the first days after infection (El-kereamy *et al.* 2011). The induction of *PpPR10* and *PpTLP-1* in both resistant and susceptible genotypes is indicative of their participation in an early response of *P. persica*, which is not sufficient to confer resistance against pathogens. The up-regulation of these PR proteins in susceptible plants, together with other components of the basal plant defence machinery described before, also indicates that the host is recognizing *T. deformans* most probably through the so-called pathogen-associated molecular patterns like β-glucans by pattern recognition receptors (Macho & Zipfel 2006). By contrast, *PpDfn1*, which was differentially induced in the resistant genotype, has been previously cloned, and it was demonstrated that the product of this gene inhibits the germination of various fungal pathogens (Wisniewski *et al.* 2003). Similarly, PpDfn1 may have functional activity against *T. deformans*. Thus, the lack of induction of *PpDfn1* correlates with *P. persica* susceptibility to the fungus.

The time course evaluation of PR proteins may also provide information concerning mechanisms operating in the pathogen. *U. maydis*, one of the most studied biotrophic fungi infecting maize, suppresses early maize response genes after initial activation (Doehlemann *et al.* 2009). On the other hand, the hemibiotrophic fungus *Colletotrichum graminicola* does not offset host defences during the biotrophic phase (Vargas *et al.* 2012). Here, a non-uniform response was observed, with a more pronounced tendency of defence repression in the

susceptible genotypes. On one hand, *PpLTP1* is dramatically reduced upon pathogen infection in the three genotypes (Fig. 3), while other PR genes are depressed only in susceptible genotypes (i.e. *PpDfn1* in DS and FL) and a further group shows early peaks of induction followed by restoration of normal levels of transcripts (i.e. *PpPAL1* in susceptible genotypes). Once again, these results highlight the particularities of the pathosystem under study.

Some metabolites related to plant defence, such as Pro (Szabados & Savouré 2009), chlorogenic acid (Fuchs & Spiteller 1998) and spermidine (Walters 2003), were also induced in all genotypes in early and/or later phases (Figs 5 & 7) after inoculation; nevertheless, their induction seems to be insufficient to confer resistance to the disease because they are also induced in susceptible genotypes. It is interesting to note that while increases in *PpP5CS1* in DS and also of *PpδOAT* in DR may explain the early rise in Pro content when facing the yeast form of the fungus (Fig. 8), the increase of this amino acid in FL may be controlled by other enzymes such as proline dehydrogenase (Qamar *et al.* 2015). Moreover, a second peak of Pro was detected in DR at 72 h.p.i. when the filamentous form of *T. deformans* is detected. In this case, this peak parallels with that of *PpP5CS2* and could have an impact on the defence responses against *T. deformans* (Figs 8 & 9). In *Arabidopsis*, different genes involved in Pro metabolism are induced depending on the type of interaction (virulent, avirulent or non-host pathogen infection), with the *AtP5CS2* gene mediating P5C and Pro contents under Avr-R and non-host interactions (Qamar *et al.* 2015).

The early peak of carotenoid induction in the three genotypes and of anthocyanins in DR and FL (Fig. 4) may contribute to the general defence process in *P. persica*. Carotenoids provide high antioxidant activities and as such are effective in dealing with pathogen-induced ROS production. Anthocyanins have also been related to plant defence (Schaefer *et al.* 2008). In this respect, the general decrease in total phenolics during the first 24 h.p.i. is rather surprising. The following increase in phenolics could contribute to the defence, as accounted by increases in flavonoids, benzoic acid and chlorogenic acid as well (Figs 4 & 5).

The analysis of total phenolics, flavonoids and *PpPAL1* performed here indicates that secondary metabolites are

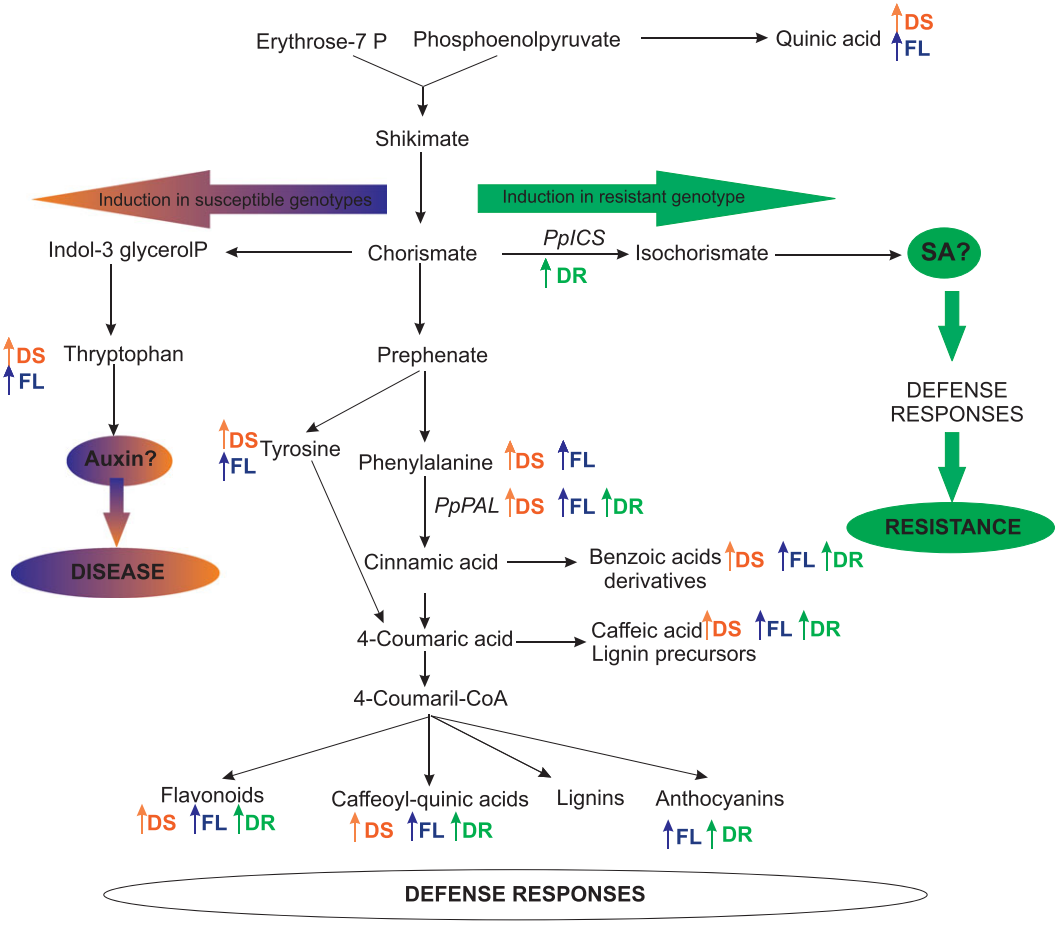

Figure 9. Schematic representation of the early response of susceptible and resistant peach genotypes to *Taphrina deformans* inoculation. Principal metabolites related to the shikimic acid pathway whose result is modified in *Prunus persica* upon *T. deformans* inoculation are shown, along with the enzymes whose transcripts were studied. Phenolic compounds and transcript induction are shown, indicating the genotype in which the modification is presented in at least one opportunity during the course of experiment. Only statistically significant changes are indicated. Auxin and salicylic acid are indicated with '?' because they were not measured in this work. [Colour figure can be viewed at wileyonlinelibrary.com]

important elements in the defence responses against *T. deformans*. Future studies will be focused on the analysis of particular secondary metabolites induced in *P. persica* when challenged with the fungus and in the elucidation of their role in this interaction.

Metabolomics of *Prunus persica* leaves reveals biphasic responses upon *Taphrina deformans* inoculation and different profiles in the resistant and susceptible genotypes

Metabolic profiling of *P. persica* leaves revealed common and distinct responses to *T. deformans* in susceptible and resistant genotypes. Metabolomics also disclosed biphasic responses in all cases, a fact that is likely corresponding to the presence of either of the two forms of the fungus, the inoculated yeast form and the later mycelial development (Fig. 1). PCA (Fig. 4) depicts a clear separation, based on their metabolic profiles, between the resistant and susceptible genotypes challenged with *T. deformans* for a period of 120 h. These results on denote, one hand, differential host modulation of primary and intermediary metabolism to halt fungal spread and on the other hand differential fungal load that perturbs plant metabolism to different extents, depending on the genotype.

In susceptible genotypes, the similar magnitude of increase in Glu, Asp and its derivative Thr, accompanied by increases in other amino acids derived from pyruvate (Ile, Val and Ala) and glycerate (Ser) in pathogen-challenged leaves, suggests these amino acids might function as N resource for the growing pathogen. Increases in these amino acids have similarly been described in other pathosystems involving biotrophic fungi. The patterns of Met, Arg, Trp, Tyr, Phe, Pro and Orn accumulation are a general feature of pathogenesis (Parker *et al.* 2009); nevertheless, they could also be used as N source for the pathogen. *T. deformans* encodes several putative amino acids transporters (TAPDE_002618g.01, TAPDE_003704g.01, TAPDE_000578g.01, TAPDE_002447g.01, TAPDE_002941g.01 and TAPDE_003537g.01) that may allow the uptake of these amino acids. In other pathogenic fungi such as *U. maydis* (Lanver *et al.* 2014), *Magnaporthe oryzae* (Oh *et al.* 2008) and *Uromyces fabae* (Struck *et al.* 2004), the fungal up-regulation of transporters that enable nutrient uptake (amino acid and peptide transporters) has been observed during the biotrophic phase. Therefore, amino acids and peptides are likely to be nutrients for fungal growth and development during the early stages of colonization.

The increased amounts of glucose can serve not only as a source of energy but also as a carbon source for fungal cell wall building because this sugar is the main component of the cell wall of the yeast form of *T. deformans* (Petit & Schneider 1983). Galactose and rhamnose are additional components of fungal cell wall, and they also increase upon infection (Figs 5 & 7). Other metabolites, such as the sugars sucrose and fructose, the alcohol glycerol and the organic acid malate (12 h.p.i.), that also may support yeast growth also rise early after inoculation (Fonseca & Rodriguez, 2011). In this respect, in *U. maydis*, the induction of a high-affinity sucrose transporter during filament and appressorium formation is a key virulence factor required for biotrophic growth (Wahl *et al.* 2010; Lanver *et al.* 2014). These results are consistent with a biotrophic behaviour in which *T. deformans* establishes a dynamic relationship with host cells that provide the nutrients to maintain the fungal development and reproduction. Some clues regarding *T. deformans* adaptation to its host *P. persica* can be found analysing the fungus genome, as genes involved in plant cell wall hydrolysis (cellulase, xylanase, cutinases and other proteases), secondary metabolism, glyoxylate cycle, detoxification, sterol biosynthesis can all be detected. In addition, its genome encodes most of the enzymes involved in primary metabolism (citric acid, glycolysis, biosynthesis of amino acids and lipid metabolism) and response to oxidative stress as well as key factors to ensure invasion and proliferation in plant tissue (Cissé *et al.* 2013).

Asparagine is conspicuously increased largely than the other amino acids (Figs 5 & 7). Asn may have different roles in the pathogenesis:

(a) it could act as a nitrogen source for the yeast form of the fungus because it increases only when the yeast is present. In addition to amino acids transporters, *T. deformans* genome also harbours an asparaginase (TAPDE_002171g.01) to metabolize Asn. In fact, it is reported that this species assimilates Asn (Moore 2011).

(b) It may induce *T. deformans* dimorphism, as in the case of *Aureobasidium pullulans* for which Asn has been demonstrated to have a direct influence in the yeast–mycelium dimorphism (Park 1982).

(c) Asn may activate PR genes. Studying the pathosystem *Pisum sativum–Nectria haematococca*, Yang *et al.* (2005) proposed this amino acid as an inductor of the expression of a fungal virulence gene (*pelD*) that allows fungal proliferation and development. Here in the case of *P. persica–T. deformans*, the increase in Asn relative levels also seem to be related to fungal pathogenesis because Asn does not increase in the resistant genotype (DR). It remains to be elucidated whether this amino acid triggers *T. deformans* dimorphism and/or pathogenesis.

Another metabolite that warrants attention is Trp, which in both susceptible plants (DS and FL) exhibits two peaks of induction (Figs 5 & 7). Trp is the precursor for the synthesis of the hormone auxin, phytoalexins and indole alkaloids. The symptoms of the disease (hyperplasia and tissue curling) have been related to a leaf hormonal imbalance caused by the fungus. Consistent with increased levels of indole-3-acetic acid (IAA) in infected tissue (Raggi 1995) are the greater levels of Trp that could support the induced synthesis of auxins during pre-symptomatic stages of the disease. In this respect, the analysis of the *T. deformans* genome allowed the identification of the genes *Tam* and *Iad* encoding putative Trp aminotransferase and indole-3-acetaldehyde dehydrogenase, respectively, which at least in *U. maydis* are involved in IAA biosynthesis (Cissé *et al.* 2013). Thus, *T. deformans* appears to manipulate plant cell metabolism in susceptible genotypes to support increased IAA synthesis. It is not clear yet, however, whether the source of IAA is the host cell, the fungus or both.

Ornithine is a precursor of polyamine biosynthesis in the reaction catalysed by ornithine decarboxylase (ODC), which converts it to putrescine. In various dimorphic fungi, such as *U. maydis* (Guevara-Olvera *et al.* 1997) and *Yarrowia lipolytica* (Jiménez-Bremont *et al.* 2001), levels of putrescine higher than those necessary to sustain vegetative growth are required for the dimorphic transition; and transition to the mycelial form depends on the fungal ODC activity. The *T. deformans* genome sequence revealed the presence of a gene encoding ODC (TAPDE_002031g.01). The Orn profile (Fig. 7) could be explained in terms of a yeast Orn demand by ODC to synthetize putrescine that leads to a net early decrease in the free amino acid in the leaf. The same Orn variation pattern was observed in both resistant and susceptible genotypes, in agreement with transition to the filamentous form in all cases (Fig. 1).

It is additionally worth discussing that raffinose, and its precursor galactinol, distinctively accumulated in a concerted manner in susceptible plants upon *T. deformans* inoculation (Figs 5 & 7). Galactinol and raffinose have been postulated to protect plant tissues from abiotic stresses (Nishizawa *et al.* 2008) while raffinose has additionally been proposed to function as a signalling molecule (ElSayed *et al.* 2013). Moreover, a role of these compounds in biotic interactions is starting to emerge; that is, galactinol has been suggested as a signalling component of the induced systemic resistance in cucumber plants (Kim *et al.* 2008). Nevertheless, in the case of *P. persica–T. deformans* interaction, if the role of raffinose were to be involved in defence mechanisms, it would be expected to also increase in the resistant genotype upon fungal inoculation. Another possibility is that raffinose serves as substrate for *T. deformans* development. Although it has been reported that *T. deformans* does not use raffinose as substrate for growth (Fonseca & Rodriguez 2011), other species with the genus *Taphrina* do. In addition, the *T. deformans* genome encodes for a gene involved in raffinose catabolism (TAPDE_002196g.01, http://genome.jgi.doe.gov/pages/search-for-genes.jsf?organism=Tapde1_1; CCG82303.1, http://www.ebi.ac.uk/ena/data/view/CCG82303, encoding a putative SIP2). In addition, no sequences for genes involved in raffinose synthesis were found in the *T. deformans* genome. Considering that *T. deformans* is a dimorphic fungus and that *in vitro* experiments are conducted with the yeast form, the possibility that *T. deformans* uses raffinose when infecting host tissue and/or when changing to its filamentous form cannot be excluded. In fact, nothing is known concerning substrate utilization and carbon source sequestration by the *T. deformans* when growing in *P. persica* leaves. Thus, the increase in raffinose could be an indicator that plant metabolism has been manipulated by the fungus. The absence of genes encoding RS in the fungus genome indicates that the increase in raffinose detected in susceptible leaves upon infection is due to a host synthesis and not due to the pathogen. In addition, other interesting points to highlight are the differences in gene expression among genotypes. In the susceptible genotype FL, increased levels of raffinose seem to be related to the significant decrease in *PpSIP2* involved in raffinose catabolism (Fig. 8). Previously, it has been reported that in heat-treated peach fruit the levels of transcripts of the catabolizing enzyme correlates with raffinose accumulation (Lauxmann *et al.* 2014). On the other hand, in the susceptible genotype DS, raffinose accumulation seems to be related to the expression of both *PpRS* (its increase at 12 h.p.i. precedes raffinose peak at 24 h.p.i.) and *PpSIP1-2*, which are induced at 72–96 h.p.i. when raffinose decreases (Fig. 8). In this respect, accumulation of transcripts encoding RS have been previously shown to correlate with an increase in raffinose (Saito & Yoshida 2011; Egert *et al.* 2013). These differences in the responses among genotypes also reinforce the hypothesis that synthesis of raffinose is not part of a defence strategy of *P. persica*.

Taken together, in inoculated susceptible leaves, the biphasic lifestyle of the fungus and the waveish modifications in both metabolites and in the defence mechanisms fit into the following model. Peaks of increases of many amino acids, organic acids and sugars precede or overlap with the first maximum of *T. deformans* when it is present in its yeast form. Therefore, these metabolites might function as nutrients to feed the fungi. The yeast form induces non-host biochemical changes as callose deposition and HR. In addition, early increases in *PpTLP1*, *PpPAL1*, *PpPR10*, anthocyanins, carotenoids, chlorogenic acid and benzoate, among others, accompany this process. At this stage, Asn may activate PR genes in *T. deformans* whose effects may be appreciated later. After 48 h.p.i., *T. deformans* turns into its filamentous form. Even though this is the parasitic from of the fungi, during the transition to the hyphae and early after, *T. deformans* may be more susceptible to plant defences (PpDfn1, PpPR10, total phenolics and flavonoids) as accounted for a decrease in the quantification of *T. deformans* at 72 h.p.i. After that, fungal load rises again, accompanied with smaller increases in amino acids and organic acids, which turned to re-establish the plant homoeostasis to set up the biotrophic lifestyle. At this stage, the secretion of lytic enzymes by the pathogen alters the interface of the fungus–leaf cell wall, allowing fungal growth. Future studies should encompass the effector proteins expressed by the fungal cells, which contribute to fungal pathogenesis and which are not known at present.

Differential features occurring in the resistant genotype when challenged with *Taphrina deformans*

Although it has been reported that resistance to *T. deformans* is a polygenic trait (Padula *et al.* 2008), little is known about *P. persica–T. deformans* interactions at the molecular and biochemical levels, and no information is available regarding the mechanisms involved in the resistance. Confocal microscopy examination of *P. persica* leaves inoculated with *T. deformans* in its yeast phase revealed fungal dimorphism, regardless of the plant genotype (Fig. 1). Thus, the resistance to *T. deformans* can be attributed to molecular and biochemical mechanisms that restrain further hypha proliferation and/or the development of the disease and not to fungal dimorphism avoidance.

One layer of defence that pathogens face is the production of compounds with anti-pathogenic properties such as phenolic compounds and ROS (Heller & Tudzynski 2011). In this respect, DR displays an earlier induction of superoxide production than susceptible genotypes (Supporting Information Fig. S2). In addition, DR plants present higher levels of flavonoids than FL and DS, before and after being challenged with *T. deformans* (Fig. 4). In addition, DR is the only genotype that exhibits a net increase in total phenolics with respect to 0 h.p.i. This peak at 96 h.p.i. matches with that of flavonoids at 96 h.p.i., indicating that flavonoids are, at least, contributing to the increase in total phenolics accumulation (Fig. 4). Moreover, *PpPAL1* transcript accumulation occurs at 72 h.p.i. in DR and precedes the rise in flavonoids (Fig. 3). In concordance with these results, higher levels of phenolic compounds were measured in leaves of a tolerant advanced peach tree selection in comparison with very susceptible trees (Padula 2010). Here, the fact that *T. deformans* charge diminishes at 96 h.p.i., after reaching maximum levels at 72 h. p.i. (Fig. 2), certainly denotes the participation of these compounds in the defence against *T. deformans*, and it could account, at least in part, for the resistance to the disease. It remains to be elucidated whether the increase in flavonoids is due to enhanced synthesis of the same pre-existing flavonoids or due to the induced synthesis of a different type.

Another differential response is the exclusive up-regulation of *PpICS* in DR (Fig. 3). Interestingly, up-regulation of *PpDfn1* at 48 h.p.i. (Fig. 3) in DR when hyphae start development in the inoculated tissue (Fig. 1) and up-regulation of *PpPAL1* are independent of SA pathway because their increase occurs before the rise in *PpICS* (Fig. 3). SA is thought to be essential for inducing resistance against biotrophic pathogens (Glazebrook 2005), and this would be the case for the DR genotype. For comparison, in other pathosystems, the infection of susceptible maize with *U. maydis*, which conducts to the development of the typical disease tumours, was not accompanied by a significant induction of SA-dependent pathways, as one of its markers PR1 was not detected early after infections and poorly detected later on (Doehlemann *et al.* 2008). SA treatment of the host plant before *U. maydis* inoculation prevents the proliferation of the fungus (Djamei *et al.* 2011). Moreover, *U. maydis* possesses a salicylate hydroxylase, which is up-regulated during its biotrophic stages and that could decrease the SA content (Rabe *et al.* 2013).

In addition, xylose makes a significant contribution to PC1 (Fig. 6, Supporting Information Table S2) and exhibits a different behaviour in DR than in the susceptible genotypes (Figs 5 & 7). Variations in the quantity of xylose in the cell wall have been related to resistance/susceptibility to pathogens (Sánchez-Rodríguez *et al.* 2009). In plants, xylose is a central constituent of hemicellulose in the cell wall, which is incorporated to this fraction as UDP-Xyl synthesized from UDP-Glc (Harper & Bar-Peled 2002). Therefore, increased free xylose in DR upon inoculation is not indicative of exacerbated cell wall biosynthesis. Nevertheless, it would be interesting to analyse the cell wall composition in the different genotypes to seek for differences. Most of the data presented show that upon pathogen *T. deformans* inoculation, the shikimic acid pathway is activated in both resistant and susceptible genotypes (Fig. 9). Shikimate is the precursor of Phe, Tyr, Trp, auxins, SA, lignin, flavonoids and other phenylpropanoids. Chorismate is a central node in the synthesis of aromatic amino acids and secondary metabolites. On one hand, the phenylpropanoid route is induced in all genotypes, as accounted by increases in relative accumulation of *PpPAL1* and some of the following compounds: Phe, Tyr, total phenolics, flavonoids, chlorogenic acid (Figs 4, 5 & 7). On the other hand, chorismate may follow divergent branches. While the SA production is activated in the resistant genotype (DR), accounted for by rises in *PpICS* (Fig. 3), the indole pathway is up-regulated in the susceptible genotypes as supported by the dramatic increase in Trp in FL and DS. Therefore, while induction of SA may conduct to activation of a cascade of defence responses in DR, the induction of the indole pathway in susceptible plants may support auxin biosynthesis in the infected tissue, leading to the development of hypertrophy and hyperplasia, both symptoms of the disease (Fig. 9). In this respect, an interesting point to highlight is that SA was identified as a repressor of auxin signalling (Wang *et al.* 2007); thus, any increase in SA in DR would also contribute to the prevention of hyperplasia development. Therefore, in future studies, it would be of interest to elucidate the responses triggered by SA in *P. persica*.

CONCLUSION

This is the first time that early events in the *T. deformans*–*P. persica* interaction are characterized and that fungal dimorphism is achieved under laboratory conditions. On one hand, our results reveal a biphasic re-programming of plant tissue in susceptible genotypes, with a first stage to provide metabolites that allow the reproduction of the yeast phase and, the second, the development of the hyphae. On the other hand, the presence of different responses such as ROS, cell death, callose deposition, induction of proline and chlorogenic acid accumulation is observed independently of the genotype analysed. Regarding the tolerant genotype, *P. persica*, resistance to *T. deformans* appears to be regulated by a complex defence network involving SA and a set of defence proteins (i.e. PpDFN1) and metabolites. Knowledge obtained here will help in the engineering of strategies to develop novel resistant genotypes to be used in breeding programmes. Availability of tolerant cultivars is important not only for the economy but also for the environment because a reduction of the considerable amounts of fungicides currently used to control this pathogen could be achieved.

CONFLICT OF INTEREST

The authors have no conflicts of interest to declare.

ACKNOWLEDGMENTS

L.A.S, C.A.B, M.F.D, G.L.M. and M.V.L. are members of the Researcher Career of CONICET. C.A.B. was a recipient of a fellowship from the Alexander von Humboldt Foundation at

A.R.F. We thank Prof. Dr E. Bellini and Dr E. Giordani [Dipartimento di Scienze Produzioni Agroalimentari e dell'Ambiente (DISPAA), Universita di Firenze] for providing *P. persica* selections DOFI-84.364.089 and DOFI-84.364.060. This work was supported by Agencia Nacional de Promoción de Actividades Científicas y Técnicas (PICT 2012-1376). INTA supported the *P. persica* collection at EEA San Pedro (PNFRU 1105062; REDGEN 1137021; PReT 127128).

REFERENCES

Bari R. & Jones J.D. (2009) Role of plant hormones in plant defense responses. *Plant Molecular Biology* **69**, 473–488.

Bassi M., Conti G. & Barbieri N. (1984) Cell wall degradation by *Taphrina deformans* in host leaf cells. *Mycopathologia* **88**, 115–125.

Bellini E., Giordani E., Perria R. & Paffetti D. (2002) Leaf curl in peach: new resistant genotypes and molecular markers. *Acta Horticulturae* **592**, 649–653.

Cantín C.M., Moreno M.A. & Gogorcena Y. (2009) Evaluation of the antioxidant capacity. *Journal of Agricultural and Food Chemistry* **57**, 4586–4592.

Chen X.-Y. & Kim J.-Y. (2009) Callose synthesis in higher plants. *Plant Signaling & Behavior* **4**, 489–492.

Cissé O.H., Almeida J.M.G.C.F., Fonseca A., Kumar A.A., Salojärvi J., Overmyer K., Hauser P.M. & Pagni M. (2013) Genome sequencing of the plant pathogen *Taphrina deformans*, the causal agent of peach leaf curl. *MBio* **4**, e00055–e00013.

Çmen I. & Ertugrul B.B. (2007) Determination of mycoflora in almond plantations under drought conditions in Southeastern Anatolia Project Region, Turkey. *Plant Pathology Journal* **6**, 82–86.

Djamei A., Schipper K., Rabe F., Ghosh A., Vincon V., Kahnt J., Osorio S., Tohge T., Fernie A.R., Feussner I., Meinicke P., Stierhof Y.D., Schwarz H., Macek B., Mann M. & Kahmann R. (2011) Metabolic priming by a secreted fungal effector. *Nature* **478**, 395–398.

Doehlemann G., van der Linde K., Aßmann D., Schwammbach D., Hof A., Mohanty A., Jackson D. & Kahmann R. (2009) Pep1, a Secreted Effector Protein of Ustilago maydis, Is Required for Successful Invasion of Plant Cells. *PloS Pathogens* **5**, e1000290.

Doehlemann G., Wahl R., Horst R.J., Voll L.M., Usadel B., Poree F., … Kämper J. (2008) Reprogramming a maize plant: transcriptional and metabolic changes induced by the fungal biotroph *Ustilago maydis*. *Plant Journal* **56**, 181–195.

Egert A., Keller F. & Peters S. (2013) Abiotic stress-induced accumulation of raffinose in *Arabidopsis* leaves is mediated by a single raffinose synthase (RS5, At5g40390). *BMC Plant Biology* **13**, 218.

El-kereamy A., El-sharkawy I., Ramamoorthy R., Taheri A., Errampalli D., Kumar P. & Jayasankar S. (2011) *Prunus domestica* pathogenesis-related protein-5 activates the defense response pathway and enhances the resistance to fungal infection. *PloS One* **6**, e17973.

ElSayed A.I., Rafudeen M.S. & Golldack D. (2013) Physiological aspects of raffinose family oligosaccharides in plants: protection against abiotic stress. *Plant Biology* **16**, 1–8.

Fernie A.R., Aharoni A., Willmitzer L., Stitt M., Tohge T., Kopka J., et al. (2011) Recommendations for reporting metabolite data. *The Plant Cell* **23**, 2477–2482.

Ferreira R.B., Monteiro S., Freitas R., Santos C.N., Chen Z., Batista L.M., … Teixeira A.R. (2007) The role of plant defence proteins in fungal pathogenesis. *Molecular Plant Pathology* **8**, 667–700.

Fonseca A. & Rodrigues M.G. (2011) *Taphrina* Fries, in: C.P. Kurtzman, J.W. Fell, T. Boekhout (Eds.), *The Yeasts, a Taxonomic Study*, fifth ed., Elsevier, The Netherlands, pp. 823–858.

Fuchs C.T. & Spiteller G. (1998) Accumulation of caffeoyl-D-quinic acids and catechins in plums affected by the fungus *Taphrina pruni*. *Zeitschrift für Naturforschung* **53c**, 799–805.

Giordani E., Giuseppe P. & Raddice S. (2013) Compared anatomy of young leaves of *Prunus persica* (L.) Batsch with different degrees of susceptibility to *Taphrina deformans* (Berk.) Tul. *Journal of Phytopathology* **161**, 190–196.

Glazebrook J. (2005) Contrasting mechanisms of defense against biotrophic and necrotrophic pathogens. *Annual Review of Phytopathology* **43**, 205–227.

Gohari A.M., Ware S.B., Wittenberg A.H.J., Mehrabi R., M'Barek S.B., Verstappen E.C.P., … Kema G.H.J. (2015) Effector discovery in the fungal wheat pathogen *Zymoseptoria tritici*. *Molecular Plant Pathology* **16**, 931–945.

Guevara-Olvera L., Xoconostle-Cázares B. & Ruiz-Herrera J. (1997) Cloning and disruption of the ornithine decarboxylase gene of *Ustilago maydis*: evidence for a role of polyamines in its dimorphic transition. *Microbiology* **143**, 2237–2245.

Harper A.D. & Bar-Peled M. (2002) Biosynthesis of UDP-xylose. Cloning and characterization of a novel *Arabidopsis* gene family, UXS, encoding soluble and putative membrane-bound UDP-glucuronic acid decarboxylase isoforms. *Plant Physiology* **130**, 2188–2198.

Heller J. & Tudzynski P. (2011) Reactive oxygen species in phytopathogenic fungi: signaling, development, and disease. *Phytopathology* **49**, 369–390.

Jiménez-Bremont J.F., Ruiz-Herrera J. & Domínguez A. (2001) Disruption of gene Y/ODC reveals absolute requirement of polyamines for mycelial development in *Yarrowia lipolytica*. *FEMS Yeast Research* **1**, 195–204.

Kim M.S., Cho S.M., Kang E.Y., Im Y.J., Hwangbo H., Kim Y.C., … Cho B.H. (2008) Galactinol is a signaling component of the induced systemic resistance caused by *Pseudomonas chlororaphis* O6 root colonization. *Molecular Plant–Microbe Interactions* **21**, 1643–1653.

Kopka J., Schauer N., Krueger S., Birkemeyer C., Usadel B., Bergmuller E., … Steinhauser D. (2005) GMD@CSB. DB: the Golm metabolome database. *Bioinformatics* **21**, 1635–1638.

Lanver D., Berndt P., Tollot M., Naik V., Vranes M., Warmann T., Munch K., Rossel N. & Kahmann R. (2014) Plant surface cues prime *Ustilago maydis* for biotrophic development. *PLoS Pathogens* **10**, e1004272.

Lauxmann M.A., Borsani J., Osorio S., Lombardo V.A., Budde C.O., Bustamante C.A., … Lara M.V. (2014) Deciphering the metabolic pathways influencing heat and cold responses during post-harvest physiology of peach fruit. *Plant, Cell & Environment* **37**, 601–616.

Lo Presti L., Lanver D., Schweizer G., Tanaka S., Liang L., Tollot M., … Kahmann R. (2015) Fungal effectors and plant susceptibility. *Annual Review of Plant Biology* **66**, 513–545.

Macho A.P. & Zipfel C. (2006) Plant PRRS and the activation of innate immune signaling. *Molecular Cell* **54**, 263–272.

Mc Donald M.C., Mc Donald B.A. & Solomon P.S. (2015) Recent advances in the *Zymoseptoria tritici*–wheat interactions: insights from pathogenomics. *Frontiers in Plant Science* **6**, 102.

Mehrotra R.S. & Aneja K.R. (1990) Ascomycotina. In *An Introduction to Mycology*, pp. 288–289. New Age International (P) Limited, Publishers, New Delhi.

Mix A.J. (1935) The life history and cytology of *Taphrina deformans*. *Phytopathology* **25**, 41–66.

Moore R.T. (2011) Lalaria. In *The Yeasts: A Taxonomic Study* (eds Kurtzman C., Fell J.W. & Boekhout T.), Fifth edn, pp. 582–591. Elsevier.

Müller G.L., Drincovich M.F., Andreo C.S. & Lara M.V. (2010) Role of photosynthesis and analysis of key enzymes involved in primary metabolism throughout the lifespan of the tobacco flower. *Journal of Experimental Botany* **61**, 3675–3688.

Nadal M., García-Pedrajas M.D. & Gold S.E. (2008) Dimorphism in fungal plant pathogens. *FEMS Microbiology Letters* **284**, 127–134.

Nishizawa A., Yabuta Y. & Shigeoka S. (2008) Galactinol and raffinose constitute a novel function to protect plants from oxidative damage. *Plant Physiology* **147**, 1251–1263.

Oh Y., Donofrio N., Pan H., Coughlan S., Brown D., Meng S., Mitchell T. & Dean R. (2008) Transcriptome analysis reveals new insight into appressorium formation and function in the rice blast fungus Magnaporthe oryzae. Genome Biology 9 R85.

Padula G. (2010) Suscettibilità a *Taphrina deformans* (Berk.) Tul. in pesco: Variabilità, ereditarietà e marcatori morfologici e biochimici. Florence, Italy, University of Florence, PhD Thesis.

Padula G., Bellini E., Giordani E. & Ferri A. (2008) Further investigations on the resistance to leaf curl (*Taphrina deformans* Berk. Tul.) of peach cultivars and F1 progenies. In *Atti del VI Convegno Nazionale Sulla Peschicoltura Meridionale* (eds Di Vaio C., Damiano C. & Fideghelli C.), pp. 113–119. Imago Media Editrice, Dragoni.

Petit M. & Schneider A. (1983) Chemical analysis of the wall of the yeast from of *Taphrina deformans*. *Achieves in Microbiology* **13**, 141–146.

Pscheidt J.W. (1995) Leaf curl. In *Compendium of Stone Fruits Diseases* (eds Ogawa J.M., Zehr E.I., Bird G.W., Ritchie D.F., Uriu K. & Uyemoto J.K.), pp. 19–20. APS Press, St. Paul., USA.

Qamar A., Mysore K.S. & Senthil-Kumar M. (2015) Role of proline and pyrroline-5-carboxylate metabolism in plant defense against invading pathogens. *Frontiers in Plant Science* **6**, 503.

Park D. (1982) Amino acid nutrition and yeast-mycelial dimorphism in *Aureobasidium pullulans*. *Transactions of the British Mycological Society* **79**, 170–172.

Parker D., Beckmann M., Zubair H., Enot D.P., Caracuel-Rios Z., Overy D.P., … Draper J. (2009) Metabolomic analysis reveals a common pattern of metabolic re-programming during invasion of three host plant species by *Magnaporthe grisea*. *Plant Journal* **59**, 723–737.

Rabe F., Ajami-Rashidi Z., Doehlemann G., Kahmann R. & Djamei A. (2013) Degradation of the plant defence hormone salicylic acid by the biotrophic fungus *Ustilago maydis*. *Molecular Microbiology* **89**, 179–188.

Raggi V. (1995) CO_2 assimilation and chlorophyll fluorescence in peach leaves affected by *Taphrina deformans*. *Physiologia Plantarum* **93**, 5440–5444.
Rodrigues M.G. & Fonseca A. (2003) Molecular systematics of the dimorphic ascomycete genus *Taphrina*. *International Journal of Systematic and Evolutionary Microbiology* **53**, 607–616.
Roessner-Tunali U., Hegemann B., Lytovchenko A., Carrari F., Bruedigam C., Granot D. & Fernie A.R. (2003) Metabolic profiling of transgenic tomato plants overexpressing hexokinase reveals that the influence of hexose phosphorylation diminishes during fruit development. *Plant Physiology* **133**, 84–99.
Rossi V., Bolognesi M. & Languasco L. (2007) Influence of weather conditions on infection of peach fruit by *Taphrina deformans*. *Phytopathology* **97**, 1625–1633.
Rudd J.J. (2015) Previous bottlenecks and future solutions to dissecting the *Zymoseptoria tritici*–wheat host–pathogen interaction. *Fungal Genetics and Biology* **79**, 24–28.
Saito M. & Yoshida M. (2011) Expression analysis of the gen family associated with raffinose accumulation in rice seedlings under cold stress. *Journal of Plant Physiology* **168**, 2268–2271.
Sánchez-Rodríguez C., Estevez J.M., Llorente F., Hernandez-Blanco C., Jorda L., Pagan I., … Molina A. (2009) The ERECTA receptor-like kinase regulates cell wall mediated resistance to pathogens in *Arabidopsis thaliana*. *Molecular Plant–Microbe Interactions* **22**, 953–963.
Schaefer H.M., Rentzsch M. & Breuer M. (2008) Anthocyanins reduce fungal growth in fruits. *Natural Product Communications* **3**, 1267–1272.
Sherif S., El-Sharkawya I., Paliyathb G. & Jayasankar S. (2012) Differential expression of peach ERF transcriptional activators in response to signaling molecules and inoculation with *Xanthomonas campestris* pv. Pruni. *Journal of Plant Physiology* **169**, 731–739.
Struck C., Mueller E., Martin H. & Lohaus G. (2004) The Uromyces fabae UfAAT3 gene encodes a general amino acid permease that prefers uptake of in planta scarce amino acids. *Molecular Plant Pathology* **5**, 183–189.
Szabados L. & Savouré A. (2009) Proline: a multifunctional amino acid. *Trends in Plant Science* **15**, 89–97.
Sziràki I., Balaàzs E. & Kiràli Z. (1975) Increased levels of cytokinin and indolacetic acid in peach leaves infected with *Taphrina deformans*. *Physiological Plant Pathology* **5**, 45–50.
Tavares S., Inácio J., Fonseca A. & Oliveira C. (2004) Direct detection of *Taphrina deformans* on peach trees using molecular methods. *European Journal of Plant Pathology* **110**, 973–982.
Tsai I.J., Tanaka E., Masuya H., Tanaka R., Hirola Y., Endoh R., Sahashi N. & Kikcuhi T. (2014) Comparative genomics of *Taphrina* fungi causing varying degrees of tumorous deformity in plants. *Genome Biology and Evolution* **6**, 861–872.
Tollot M., Assmann D., Becker C., Altmüller J., Dutheil J.Y., Wegner C.-E. & Kahmann R. (2016) The WOPR protein Ros1 is a master regulator of sporogenesis and late effector gene expression in the maize pathogen *Ustilago maydis*. *PLoS Pathogens* **12**, e1005697.
van Loon L.C., Rep M. & Pieterse C.M. (2006) Significance of inducible defense-related proteins in infected plants. *Annual Review of Phytopathology* **44**, 135–162.
Vargas W.A., Sanz Martín J.M., Rech G.E., Rivera L.P., Benito E.P., Díaz-Mínguez J.M., Thon M.R. & Sukno S.A. (2012) Plant defense mechanisms are activated during biotrophic and necrotrophic development of *Colletotrichum graminicola* in maize. *Plant Physiology* **158**, 1342–1358.
Vlot A.C., Dempsey D.M.A. & Klessig D.F. (2009) Salicylic acid, a multifaceted hormone to combat disease. *Annual Review of Phytopathology* **47**, 177–206.
Wahl R., Wippel K., Goos S., Kamper J. & Sauer N. (2010) A novel high-affinity sucrose transporter is required for virulence of the plant pathogen *Ustilago maydis*. *PLoS Biology* **8**, e1000303.
Walters D.R. (2003) Resistance to plant pathogens: possible roles for free polyamines and polyamine catabolism. *New Phytologist* **159**, 109–115.
Wang D., Pajerowska-Mukhtar K., Hendrickson C.A. & Dong X. (2007) Salicylic acid inhibits pathogen growth in plants through repression of the auxin signaling pathway. *Current Biology* **17**, 1784–1790.
Wisniewski M.E., Bassett C.L., Artlip T.S., Webb R.P., Janisiewicz W.J., Norelli J.L., Goldway M. & Droby S. (2003) Characterization of a defensin in bark and fruit tissues of peach and antimicrobial activity of a recombinant defensin in the yeast, *Pichia pastoris*. *Physiologia Plantarum* **119**, 563–572.
Yang Z., Rogers L.M., Song Y., Guo W. & Kolattukudy P.E. (2005) Homoserine and asparagine are host signals that trigger *in planta* expression of a pathogenesis gene in *Nectria haematococca*. *Proceedings of the National Academy of Sciences of the United States of America* **11**, 4197–4202.
Ziosi V., Bonghi C., Bregoli A.M., Trainotti L., Biondi S., Sutthiwal S., … Torrigiani P. (2008) Jasmonate-induced transcriptional changes suggest a negative interference with the ripening syndrome in peach fruit. *Journal of Experimental Botany* **59**, 563–573.
Zubini P., Zambelli B., Musiani F., Ciurli S., Bertolini P. & Baraldi E. (2009) The RNA hydrolysis and the cytokinin binding activities of PR-10 proteins are differently performed by two isoforms of the Pru p 1 peach major allergen and are possibly functionally related. *Plant Physiology* **150**, 1235–1247.

Received 9 June 2016; accepted for publication 13 February 2017

SUPPORTING INFORMATION

Additional Supporting Information may be found online in the supporting information tab for this article.

Figure S1. Leaves of DS (DOFI-84.364.089), DR (DOFI-84.364.060) and FL (Flavorcrest) inoculated with *Taphrina deformans*. The adaxial and abaxial sides of the leaf are shown in the top and bottom rows of each series of images of each genotype.
Figure S2. Histochemical visualization of ROS. Superoxide anion accumulation was detected by vacuum infiltration of the leaves with NBT. Leaves were collected after different hours post inoculation (h.p.i.). As controls, leaves of DS genotype were mock inoculated (CDS). DS, DOFI-84.364.089; DR, DOFI-84.364.060; and FL, Flavorcrest. Abaxial side of the leaf is shown.
Figure S3. Histochemical visualization of cell death. Cell death staining was evaluated using the Evans Blue reagent. Leaves were collected after different hours post inoculation (h.p.i.). DS, DOFI-84.364.089; DR, DOFI-84.364.060; and FL, Flavorcrest. Abaxial side of the leaf is shown.
Figure S4. Expression analyses of transcripts encoding enzymes involved in plant defence responses in control leaves of *Prunus persica* during 120 h after detachment. Means (±SD) of results obtained, using three independent RNAs as template are shown. The expression level of each gene is relative to that of 0 h.p.i. *PpEF1α* was used as reference gene. For each transcript analysed, bars with the same letters are not significantly different ($P < 0.05$). Leaves of DOFI-84.364.060 (DR) were mock treated and used as controls of transcript expression stability.
Figure S5. Metabolite–metabolite correlation heat map of GC–MS data from inoculated leaves. Metabolites are grouped in modules and in the same order as in Fig. 5 and Supporting Information Table S1. Boxes represent Pearson correlation coefficient values of metabolite pairs using the scale shown at the bottom of the figure.
Table S1. Metabolites analysed by GC–MS in leaves of *Prunus persica* inoculated with *Taphrina deformans*. DR. The ratio between the levels in each sample relative to the levels in CDS (control DS) at each corresponding time is indicated. Values represent the mean of five independent determinations with their corresponding standard deviation.
Table S2. Variable contribution to the principal components (%).
Table S3. Description of primers used for quantitative real-time RT-PCR.
Table S4. Metabolite reporting guidelines (checklist table).
Table S4. Metabolite reporting guidelines (checklist table).
Table S4. Overview of the metabolite reporting list.